



Species distribution models for deep-water coral habitats that account for spatial uncertainty in trap-camera fishery data

Beau Doherty^{1,*}, Sean P. Cox², Christopher N. Rooper^{3,4}, Samuel D. N. Johnson^{1,2},
Allen R. Kronlund⁴

¹Landmark Fisheries Research, 211-2414 St. Johns Street, Port Moody, BC V3H 2B1, Canada

²Quantitative Fisheries Research Group, School of Resource and Environmental Management, Simon Fraser University, Burnaby, BC V5A 1S6, Canada

³Alaska Fisheries Science Center, National Marine Fisheries Service, 7600 Sand Point Way NE, Seattle, WA 98115, USA

⁴Pacific Biological Station, Fisheries and Oceans Canada, 3190 Hammond Bay Road, Nanaimo, BC V9T 6N7, Canada

ABSTRACT: Bottom-contact fisheries present risks to vulnerable marine ecosystems (VMEs) such as deep-water coral and sponge communities. Managing these risks requires better knowledge about VME spatial distribution within fishing areas. In this paper, we develop predictive species distribution models for alcyonacean (Order Alcyonacea) corals at SGaan Kinglas–Bowie Seamount (SK-B) in British Columbia, Canada, based on direct presence/absence observations obtained from deep-water cameras attached to commercial fishing gear. We obtained *in situ* presence/absence observations of deep-water corals (Order Alcyonacea, Order Antipatharia, Order Pennatulacea, Family Stylasteridae) and sponges (Class Hexactinellida, Class Demospongiae) at 124 locations during commercial fishing trips at the SK-B marine protected area. We developed species distribution models for alcyonacean corals at SK-B and compared the performance of models using 4 different estimators of trap landing position (surface drop position and 3 Bayesian estimators) to account for spatial uncertainty in observation locations. We found that the different estimators for landing position affected variable selection, model performance, and model predictions. The best-fitting models using the 4 different landing position estimators had mean AUC values ranging from 0.71 to 0.78 and maximum kappa values ranging from 0.36 to 0.47. This study demonstrates how collaborative research surveys with commercial fisheries can provide fine-scale spatial data for coral and sponge habitat mapping using an approach that is scalable for benthic habitat risk assessment for large, possibly remote, areas where fisheries operate.

KEY WORDS: Sensitive benthic habitats · Bottom-contact fishing · Quantitative risk assessment · Presence/absence data · Vulnerable marine ecosystems · Seamount

— Resale or republication not permitted without written consent of the publisher —

1. INTRODUCTION

Demersal fisheries targeting fish or invertebrate species living on or near the seafloor can damage sensitive benthic habitats formed by deep-water corals and sponges. These vulnerable marine ecosystems (VMEs) may be slow to recover from fishing impacts

(Sainsbury et al. 1997, Williams et al. 2010) because they are composed of slow-growing, long-lived animals that occur in isolated populations with limited larval dispersal and sporadic recruitment (Andrews et al. 2002, 2009, Mercier & Hamel 2011, Waller et al. 2014). Although fisheries are increasingly scrutinized for potential impacts on VMEs, fishing damage to

*Corresponding author: bdoherty@landmarkfisheries.com

coral and sponge habitats is rarely quantified (see examples in Dichmont et al. 2008, Welsford et al. 2014, Pitcher et al. 2015, 2017, Barnett et al. 2017), in large part due to limited information on their location.

Species distribution models (SDMs) aim to predict the location of VMEs and improve information for fisheries management and marine-use planning. SDMs use a statistical model (e.g. logistic regression, generalized additive model [GAM], random forest, boosted regression) to estimate relationships between environmental covariates and the probability of species occurrence. A fitted SDM can produce maps showing the probability of species occurrence (e.g. coral or sponge habitat) or densities over large areas where species observations are not available (Guisan & Zimmermann 2000, Woodby et al. 2009, Rooper et al. 2014). SDMs for coral habitats model relationships between coral presence/absence or abundance and environmental predictor variables such as depth, currents, temperature, fishing pressure, and bottom-substrate features (e.g. bottom type, rugosity, slope) that are often associated with high or low densities of deep-water corals (Woodby et al. 2009, Rooper et al. 2014, Wilborn et al. 2018). Estimating functional relationships for SDMs and predicting species distribution requires 3 types of information: (1) observations of presence-only, presence/absence, or abundance indices for indicator taxa; (2) environmental covariates (e.g. bottom type, depth, slope, temperature, currents) associated with each observation, and (3) environmental covariates at locations where predictions of presence/absence need to be made. The quality, quantity, spatial resolution, and observation type (e.g. presence-only, presence/absence, abundance) of these 3 kinds of information can affect the accuracy of SDMs and their usefulness for managing fishing risks on VMEs (Araújo & Guisan 2006, Anderson et al. 2016, Rowden et al. 2017, Winship et al. 2020).

The majority of SDMs for deep-water coral and sponge habitats use presence-only data from sources such as museum records, research expeditions, or fisheries bycatch, where reliable absence information is often unavailable (Vierod et al. 2014, Winship et al. 2020). Most presence-only SDMs (e.g. maximum entropy or environmental niche factor analysis) are limited to estimating a relative probability of species presence (being unbounded) with no way to estimate the proportionality to absolute probability without baseline prevalence data (Phillips & Elith 2013). Furthermore, extending to models bounded between 0 and 1 (e.g. logistic models) does not solve the issue, as the likelihood functions are identical for models whose species prevalence differs by a multiplicative

constant, rendering them indistinguishable without some baseline prevalence data (Phillips et al. 2004, Hastie & Fithian 2013, Phillips & Elith 2013, Fithian et al. 2015). While relative probabilities may be adequate for some decision-making, such as ranking areas of habitat suitability for conservation planning, absolute probabilities are often preferred (Winship et al. 2020). For example, the expected proportion of coral and sponge habitats overlapping with fishing grounds can be estimated from absolute probabilities, while relative probabilities can only identify areas that are more likely to overlap with coral and sponge habitats relative to other areas. Another limitation with presence-only methods is that they frequently suffer from large sampling bias, whereby models may incorrectly predict higher probabilities of occurrence for sites that are more frequently sampled in comparison to sites with low sampling effort (Fithian et al. 2015). For example, fisheries bycatch data may exclude more complex terrain or other unfished areas that are well suited for coral and sponge habitats. This type of bias is problematic for managing fisheries, as it can produce higher probabilities of coral habitat in the areas most fished (i.e. with higher sampling effort), leading to suboptimal management strategies that perceive greater conservation benefits from closing valuable fishing grounds than might actually be achieved. While presence-only models have useful applications, such as identifying potential VME sites for further investigation, determining potential suitable habitat distributions, informing survey design, spatial planning, and evaluating trade-offs between fisheries and conservation objectives (Davies & Guinotte 2011, Lagasse et al. 2015, Chu et al. 2019, Kinlan et al. 2020), they are less ideal for managing fishing risks to bottom habitat (Winship et al. 2020). Modelling approaches using presence/absence data are preferred because they typically have better predictive performance (e.g. less bias and greater accuracy) and provide measures of absolute probability that are easily interpreted (Phillips et al. 2009, Hastie & Fithian 2013, Guillera-Arroita et al. 2014, Fithian et al. 2015, Anderson et al. 2016, Winship et al. 2020).

For many deep-water habitats, observations of corals and sponges are most commonly available via bycatch in commercial fishing or fishery-independent surveys using bottom-contact fishing gear (Gass & Willison 2005, Watling & Auster 2005, Finney & Boutilier 2010, Rooper et al. 2014, Sigler et al. 2015). Although bycatch data provides observations over large spatial extents where fisheries operate, and are relatively inexpensive to collect, such observations have inherent limitations for species distribution mod-

elling. Bycatch data limits SDM choices to presence-only methods using simulated absence data from the study site (i.e. pseudo-absences, Phillips et al. 2009, Iturbide et al. 2015) or requires inferring absences from fishing events with unobserved bycatch. Lack of bycatch observations may not imply absence of corals or sponges within an area due to selectivity of the gear that can vary with size and morphology of the species. For example, taller species with more complex branching are more likely to be entangled with fishing gear or retained in trawl mesh, compared with smaller specimens or those that easily break apart (Auster et al. 2011, Rooper et al. 2011, Ewing et al. 2014). While the inference of absence from fishing events with zero bycatch may be a reasonable assumption for some taxa or taxonomic groups, it can underestimate prevalence of taxa with low selectivity in fishing gear.

The spatial accuracy of the bottom location from which deep-water coral and sponge observations originate may range from metres to several kilometres for different data types. For many observations, spatial accuracy is low, limiting the spatial resolution for SDMs and habitat mapping (Finney 2009, Fithian et al. 2015). For example, a coral bycatch observation taken at the surface (i.e. a physical specimen or part thereof) may have arisen from a coral colony anywhere along a trawl tow track spanning several kilometres. A common assumption applied to SDMs using bycatch trawl data is that the observation occurred at the midpoint of the tow, but the effects of this assumption on model performance are not typically evaluated. The environmental predictor information used to fit SDMs is commonly extracted from terrain attributes derived from bathymetry and backscatter multibeam data (e.g. depth, rugosity, slope, bathymetric position index [BPI], substrate), oceanographic datasets (e.g. primary production, temperature), and oceanographic models (e.g. tides, current, temperature, salinity, substrate), rather than measured *in situ* (Brown et al. 2011, Rengstorf et al. 2012). The spatial scales of the environmental data are highly variable, ranging from 0.1 to 10 km or greater for oceanographic and modelled datasets, to 1–100 m for terrain information derived from high-resolution multibeam acoustic data (for a detailed review of the environmental data available for SDMs, see: Brown et al. 2011, Winship et al. 2020). If environmental predictor data varies over finer spatial scales than the uncertainty associated with the observation location, then the predictor data used to fit the model will be inaccurate and can lead to poorer model performance (Graham et al. 2008, Naimi et al. 2011, Fithian

et al. 2015). In this case, the spatial uncertainty in observations are compounded because SDMs will include both the spatial uncertainty in the presence/absence observations (i.e. response variable) and spatial uncertainty in extracted environmental data (i.e. predictor variables) used to fit the model. While crude estimates of observation bottom locations can be acceptable for regional-scale modelling, they are likely too coarse for informing spatial fishery management on relatively fine spatial scales.

Management of fishing impacts on VMEs could be improved via spatial modelling and mapping aimed at delineating fine-scale boundaries for coral or sponge habitats (Rengstorf et al. 2012, Rowden et al. 2017). Such mapping would require relatively high-resolution observations, environmental data, and models, because coral and sponge habitats often occur in isolated small patches (Heifetz 2002), even in areas with optimal environmental features (e.g. depth and rocky substrate; Mortensen & Buhl-Mortensen 2004). For example, recent fishing closures designed to protect small glass sponge reefs (Class Hexactinellida) in Georgia Strait and Howe Sound, British Columbia (BC), have a median area of 1.1 km², with individual closures ranging from 0.6 to 7.6 km² in size. These sponge reefs have been mapped using remotely operated vehicles (ROVs), drop-cameras, SCUBA diving, and multibeam backscatter (Conway et al. 2005, Chu & Leys 2010, Clayton & Dennison 2017, Dunham et al. 2018), rather than SDMs, but they demonstrate how spatial management strategies can target specific areas of conservation concern more effectively when fine-scale resolution (e.g. 10–100 m) information on bottom habitats is available. While SDMs typically generate probability maps with coarser spatial resolution than multibeam data, fine-scale resolution SDMs are increasingly possible due to improved observational data, high-resolution multibeam bathymetry, and new modelling approaches (Dolan et al. 2008, Guinan et al. 2009, Woodby et al. 2009, Neves et al. 2014, Rooper et al. 2016). In some cases, oceanographic data at coarser resolutions can be interpolated to finer scales (Rooper et al. 2014, 2017, Georgian et al. 2019) to match the scale of SDMs needed to inform management, or SDMs may be developed using primarily high-resolution seafloor terrain covariates (Dolan et al. 2008, Woodby et al. 2009, Georgian et al. 2014, Rowden et al. 2017). The level of spatial resolution needed for effective management will depend on objectives and other factors, such as the patchiness of coral or sponge habitats, the distribution of fishing effort, and the ability to manage at finer spatial scales. Crude map-

ping of these habitats from coarse-resolution SDMs can lead to poorly designed boundaries for protecting VMEs and spatial closures that are misplaced or include large buffer zones, where a large proportion of the area contains none of the habitats in need of protection (Anderson et al. 2016, Rowden et al. 2017). Misplaced spatial closures or management decisions arising from imprecise SDMs may be counterproductive to both conservation and socioeconomic fishery objectives by shifting fishing effort into other VMEs that are undiscovered and unprotected, and/or creating unnecessary economic losses for fisheries (Penney & Guinotte 2013, Lagasse et al. 2015).

Ideally, SDMs would be estimated via presence/absence or abundance observations as might be collected from submersibles, ROVs, tow-cameras, or drop-cameras (Williams et al. 2014, Rooper et al. 2016, Rowden et al. 2017, Doherty et al. 2018) where the camera location is known with greater precision. These types of *in situ* video observations of bottom habitats are expensive to collect and are typically only available for specific areas of interest where dedicated research surveys have been conducted. Bycatch data is often the only data available for coral and sponge distributions in fishing areas, which limits model choices for SDMs and their usefulness for effective management of fishing risks on VMEs. For many fishing areas and potential VMEs, particularly for high relief areas without regular trawl surveys or trawl fisheries, bycatch data is sparse or unavailable. This is the case for the Canadian sablefish fishery that operates along the continental slope and, to a lesser extent, at offshore seamounts in BC at depths of 200–1350 m using longline hook and trap gear (see Fig. 1). To address the lack of information on potential coral and sponge habitats within sablefish fishing areas, we developed a deep-water camera system that can be deployed on sablefish fishing traps during regular fishing operations and the annual stratified random survey (Doherty et al. 2018). These camera systems provide an approach that is scalable and has the potential to be widely implemented across fisheries. They allow collection of the presence/absence and abundance observations needed for effective monitoring, mapping, and risk assessment of coral and sponge habitats within fishing footprints. If these kinds of camera systems were widely implemented during regular fishing operations, they could collect habitat data just as frequently as bycatch, but without the main limitations (e.g. presence-only observations and spatial uncertainty), and at a much cheaper cost than other alternatives for collecting *in*

situ bottom observations (e.g. ROVs, tow-cameras, submersibles). In the present paper, we describe the development of predictive SDMs for corals at the SGaan Kinglas–Bowie Seamount (SK-B) off the coast of BC (see Fig. 1), based on direct presence/absence observations obtained from the deep-water cameras attached to commercial trap fishing gear (i.e. 'trap-cameras'). The camera system was deployed opportunistically during regular fishing trips to SK-B as well as on targeted deployments according to equal stratified random (ESR) and completely random sampling strategies designed to develop, improve, and validate SDMs (Hirzel & Guisan 2002). Spatial uncertainty is taken into account for both presence/absence observations and environmental covariates used in model fitting via alternative Bayesian estimators of the camera position on the seafloor (Doherty et al. 2018).

2. MATERIALS AND METHODS

2.1. Study site

SK-B is the southernmost seamount in the Kodiak–Bowie Seamount Chain (also called the Pratt–Welker Chain) that runs 1000 km northwest from SK-B Seamount up to Kodiak Seamount, encompassing 14 major and several smaller seamounts (Turner et al. 1980, Chaytor et al. 2007). SK-B Seamount has an oblong shape oriented in the southwest–northeast direction, with a linear ridge extending approximately 20 km northeast from its northern end (Fig. 1). The slopes of SK-B Seamount extend from a base depth of approximately 2800 m up to a flat summit area of 26 km² at depths ranging from 200 m to 250 m (Chaytor et al. 2007). Several pinnacles arise from an elevated area near the centre of the summit, with the tallest pinnacle reaching 24 m depth (Halcro 2000). The average slopes on the seamount are between 10° and 20°; however, slopes on the southwest and northeast flanks are more variable, ranging from 0° to 50°, likely created by solidified lava flows (Chaytor et al. 2007). In 2008, a marine protected area (MPA) was designated around SK-B and 2 seamounts to the north (the Hodgkins and Davidson seamounts), with new zoning for fishing (Government of Canada 2008). Between 2008 and 2017, the sablefish (*Anoplopoma fimbria*) fishery by longline trap was the only fishing permitted within the SK-B Seamount MPA and was restricted to fishing in Zone 2 on SK-B at depths below the approximate 457 m contour (DFO 2015) (Fig. 1).

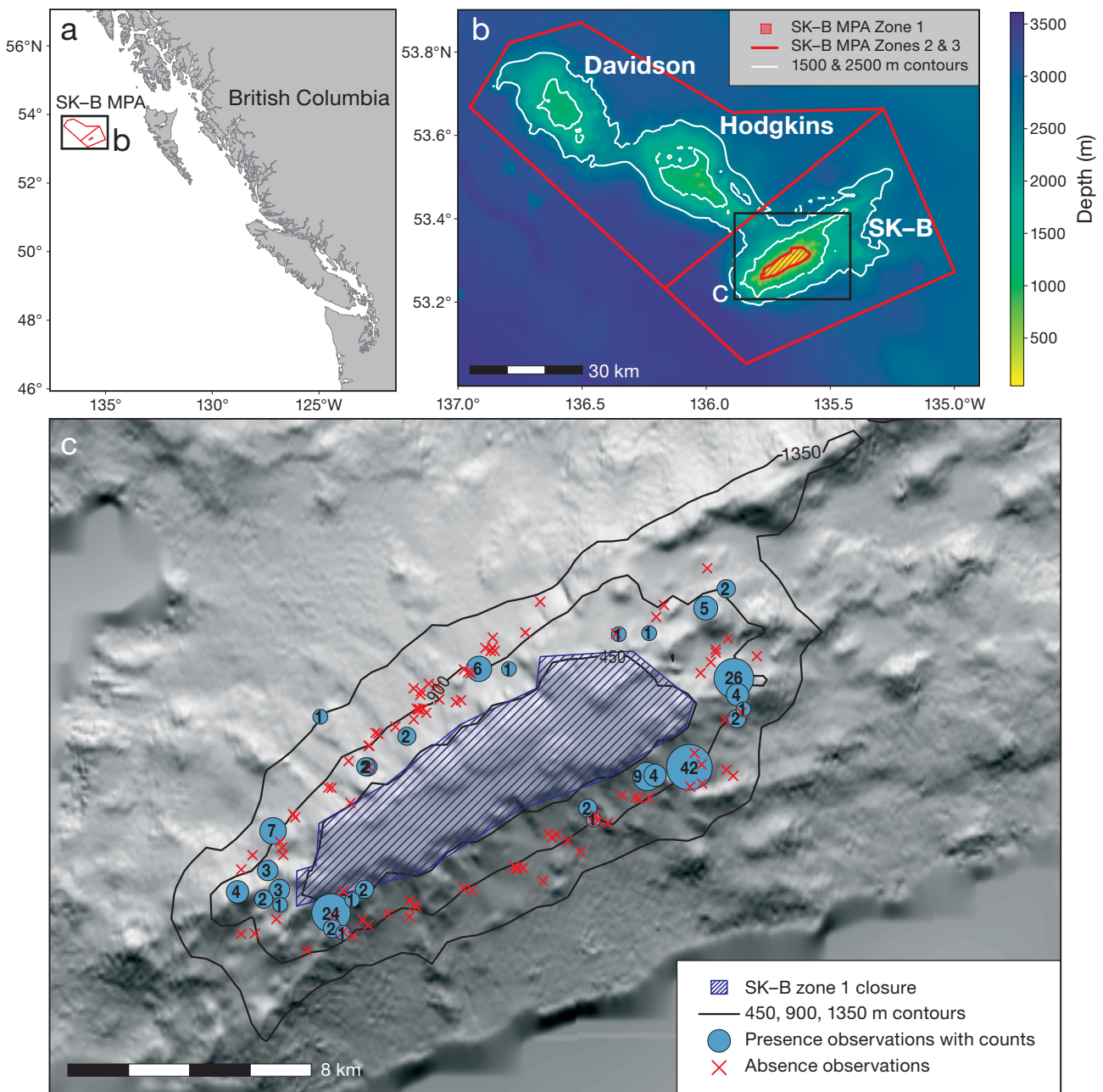


Fig. 1. (a) British Columbia coast showing location of SGaan Kinglas-Bowie (SK-B) marine protected area (MPA), (b) Davidson, Hodgkins, and SK-B seamounts within the SK-B MPA boundaries, and (c) presence/absence observations at camera drop locations. Circle sizes in (c) are proportional to unique colony counts (i.e. distinct coral stands) observed on camera deployments, which is the number shown in the circle

2.2. Sampling design

Camera systems were mounted to fishing traps during select fishing trips to SK-B from 2013 to 2017 and were programmed to record 1 min video clips at regular 2 h intervals while the trap was stationary on the bottom. Camera video recordings were also trig-

gered by an internal accelerometer during gear movement on retrieval, for impact forces greater than 0.6 g units. The trap-camera systems were deployed alongside depth-temperature sensors (Seabird SBE 39) and accelerometers (ActiGraph wGT3X-BT) in single traps on commercial bottom longline sets with 40–60 total traps. No more than 1 camera was de-

ployed per longline set, and set lengths ranged from 1.8 to 4.0 km, with a median of 2.9 km. All epifauna observed in camera videos were identified to the lowest taxonomic rank possible, which was often the Order or Family level due to limited visibility and lack of physical samples to confirm genus or species (refer to Doherty & Cox 2017 and Doherty et al. 2018 for details on species identification and images).

For the 2013–2015 sampling trips, we deployed a camera on 92 commercial fishing sets at SK-B. Fishing at SK-B has historically occurred on all sides of the seamount at depths of 250–1350 m (Canessa et al. 2003), and deployment during regular fishing sets was expected to provide relatively uniform sampling of SK-B. During the 2013–2015 sampling period, cameras were deployed as time permitted during regular fishing operations on the middle trap on the set to reduce the risk of losing cameras from lost traps. As fishing sets are generally deployed perpendicular to contour lines (shallow to deep or vice versa), deploying cameras on the middle traps led to a greater proportion of observations in the 800–1150 m depth range.

Initial SDMs fit to data collected during the 2013–2015 fishing trips identified depth, rugosity, slope, and maximum tidal speed as important predictor variables for coral habitats (Doherty 2016). In 2016, we implemented a sampling strategy to improve and validate model performance. The strategy involved: (1) ESR sampling locations for model training (Hirzel & Guisan 2002), (2) completely random sampling locations for model testing, and (3) routine commercial fishing sets where the locations were selected by the skipper. ESR sampling locations were designed to provide new training data in areas with combinations of predictor variables poorly represented by the 2013–2015 sampling. The sampling space for ESR and random sites included all areas at SK-B Seamount within the 500–1450 m depth range divided into 200 m × 200 m grid cells, including unfishered areas such as the Northeast ridge. Depths shallower than 500 m were excluded from the sampling space to avoid sample locations too close to the fishing closure, which approximately follows the 250 fathom (457 m) contour. We stratified by 4 environmental variables (depth, maximum tidal current, rugosity, and slope), and each variable was divided into 3 strata to ensure the full range of values was sampled (Table 1). Each variable/stratum combination was used to generate distinct strata layers for sampling. Theoretically, this would produce 3^4 (81) distinct strata; however, several variable/stratum combinations do not exist at SK-B or occur in a small number of grid cells. Strata with <18 grid cells were aggre-

Table 1. Environmental variables and levels used for stratification. ACR: arc:chord ratio

Variable	Levels	Range
Rugosity (ACR)	Low	1.0–1.1
	Medium	1.1–1.2
	High	1.2–1.31
Slope (°)	Low	1–21
	Medium	21–40
	High	40–60
Maximum tidal current (cm s ⁻¹)	Low	5–17
	Medium	17–28
	High	28–43
Depth (m)	Shallow	340–800
	Medium	800–1150
	Deep	1150–1505

gated into a 'combination' stratum for sampling, leading to a total of 19 distinct strata (Table 2). Some strata were sampled frequently in 2013–2015, while others had limited sampling or no sampling coverage. We proposed 21 new ESR sampling locations with the goal of obtaining at least 3 samples within each stratum for model fitting. ESR sites were randomly selected from the available grid cells within each stratum. An additional 24 sites were selected at random from the sampling space to be used as test data for assessing model performance. The random sample locations also provided unbiased estimates of coral prevalence within the 500–1450 m depth range at SK-B Seamount (i.e. the sampling space) that were used to assess candidate probability thresholds for assigning presence/absence from model outputs (Freeman & Moisen 2008a, Phillips & Elith 2013). Finally, the sampling protocol during routine commercial fishing sets (e.g. sets that were not deployed in ESR or random sites) alternated the camera position among shallow, middle, and deep ends of the set to obtain observations across all depth strata, but was otherwise unchanged. There were 32 cameras deployed in 2016 that successfully captured bottom footage: 11 at ESR sites, 14 at random sites, and 7 during regular fishing operations.

2.3. Trap location estimates

For each trap-camera observation, we used a Bayesian camera location estimator to produce a posterior grid of probabilities for the trap-camera landing position on the seafloor (Doherty et al. 2018). We used surface deployment coordinates as the centre point of an uncorrelated bivariate normal prior distribution for the bottom location of each trap-camera. The pos-

Table 2. Total trap-camera observations from 2013–2016 and proposed 2016–2017 equal stratified random (ESR) sampling sites for different habitat strata. The combination stratum includes combinations of stratification levels that occur in <18 sample sites (200 m × 200 m grid cells)

Stratum #	Habitat variables and levels in strata				Available 200 m × 200 m sample sites	Proposed 2016–2017 ESR sampling	Camera observations	
	Rugosity	Slope	Tidal current	Depth			2013–2015	2013–2016
1	Low	Medium	Low	Shallow	108	2	1	7
2	Low	Low	Medium	Shallow	161	1	2	8
3	Low	Medium	Medium	Shallow	559	0	7	12
4	Low	Low	High	Shallow	22	2	1	3
5	Low	Medium	High	Shallow	136	1	2	3
6	Low	Low	Low	Medium	282	0	12	14
7	Low	Medium	Low	Medium	803	0	32	36
8	Medium	Medium	Low	Medium	30	0	7	9
9	Medium	High	Low	Medium	20	3	0	1
10	Low	Low	Medium	Medium	113	0	5	6
11	Low	Medium	Medium	Medium	231	0	9	9
12	Medium	Medium	Medium	Medium	19	0	3	4
13	Low	Low	Low	Deep	545	0	3	3
14	Low	Medium	Low	Deep	1110	0	5	5
15	Medium	Medium	Low	Deep	66	2	1	1
16	Low	High	Low	Deep	30	3	0	0
17	Medium	High	Low	Deep	38	3	0	0
18	High	High	Low	Deep	18	3	0	0
19	Combination stratum				67	1	2	3
Total						21	92	124

terior distribution was proportional to the product of this prior with a likelihood function computed at each grid point given the depth sensor observation from the camera and a 10 m multibeam bathymetry raster (refer to Table 3 in Doherty et al. 2018 for statistical model). Posterior grid cells are re-normalized by assigning zero probability to grid cells with probability <0.01 % that occur in areas of vanishingly small density (Doherty et al. 2018).

The 2016 surface deployment coordinates for camera drops were recorded at sea, while 2013–2015 surface deployment coordinates $u^{(i)} = (\tilde{x}^{(i)}, \tilde{y}^{(i)})$ were estimated by taking a weighted average of the deployment track start and end locations, where:

$$\tilde{x}^{(i)} = x_{\text{START}}^{(i)} + \frac{n^{(i)}}{N^{(i)}} (x_{\text{END}}^{(i)} - x_{\text{START}}^{(i)}) \quad (1)$$

$$\tilde{y}^{(i)} = y_{\text{START}}^{(i)} + \frac{n^{(i)}}{N^{(i)}} (y_{\text{END}}^{(i)} - y_{\text{START}}^{(i)}) \quad (2)$$

where $N^{(i)}$ is the total number of traps on the set and $n^{(i)}$ is the position of the trap with the mounted camera-system (and depth sensor) along a straight line between the start and end positions for each set i .

The Bayesian trap location estimator was used to account for uncertainty in the trap landing position when extracting environmental raster data for SDM parameterization. We fit 4 models using different sets

of environmental data obtained from (1) the drop location (i.e. the centre point of the prior distribution), (2) the posterior mode grid cell location, (3) the posterior medoid grid cell location, and (4) a posterior-weighted average of grid cells (Fig. 2). The posterior mode uses a point estimate from the posterior grid cell with the highest posterior probability. The posterior medoid is the grid cell with non-zero probability that is closest to the cell with median x (i.e. Easting) and median y (i.e. Northing) coordinates from posterior grid cells with non-zero probabilities. Finally, the posterior probability grid was used to estimate a weighted average of the environmental predictor data from multiple grid cells, rather than using a single grid cell as a point estimate.

2.4. Response variable

Deep-water corals are commonly modelled at higher taxonomic levels that pool observations of families in the Alcyonacea order (e.g. Acanthogorgiidae, Paragorgiidae, Isididae, Plexauridae, Primnidae), as there is often insufficient taxonomic resolution in datasets to produce models at the family, genus, or species level (Woodby et al. 2009, Rooper et al. 2014, 2017). This was the case for our dataset at

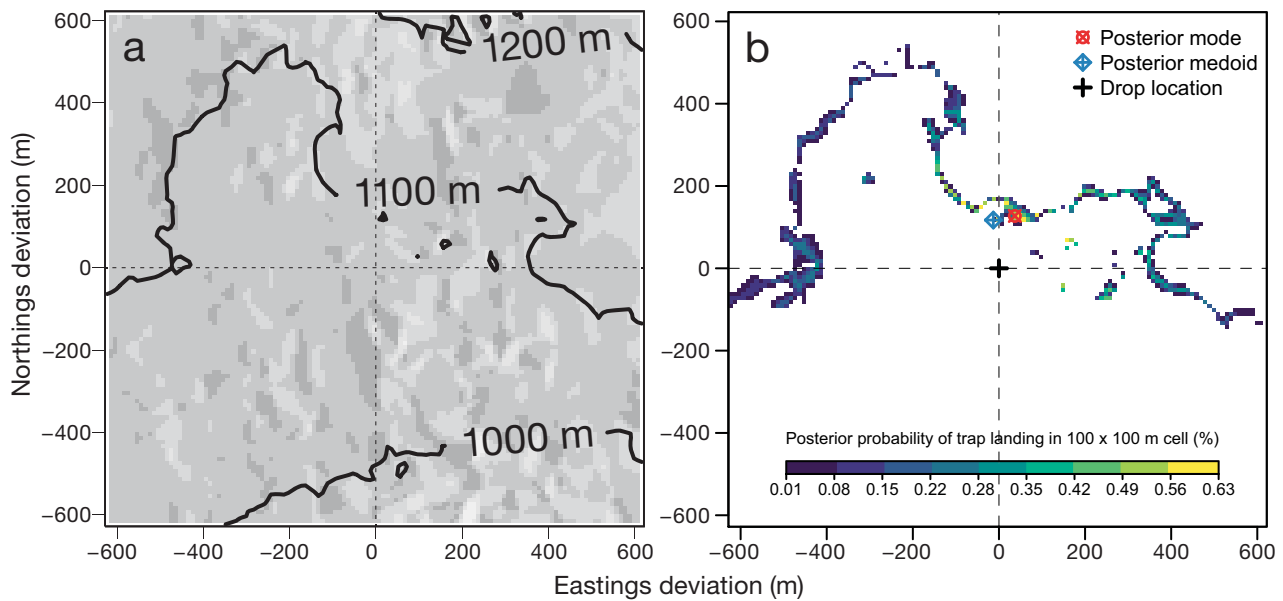


Fig. 2. An example of the Bayesian trap location estimator for one trap deployment showing (a) the $1.25 \text{ km} \times 1.25 \text{ km}$ subset of the multibeam bathymetry grid with cross hairs indicating surface drop position used as the prior mean (\tilde{x}, \tilde{y}) for the trap position and (b) the Bayes posterior grid

SK-B, and we grouped all coral observations of the Alcyonacea order together for the response variable in SDMs. The Alcyonacea order includes the majority of corals observed at SK-B, and different species are often observed in the same sampling location, indicating many alcyonacean coral species occupy similar habitats at SK-B (Doherty & Cox 2017, Gale et al. 2017). SK-B Alcyonacea observations included the families Primnoidae, Isididae, Plexauridae, Paragorgiidae, and Alcyoniidae, most of which are associated with taxa providing habitat structure (Krieger & Wing 2002, Etnoyer 2008). The exception to this is the Alcyoniidae family, with the genera *Anthomastus* and *Heteropolypus*, that are smaller in size, and commonly referred to as soft corals since they do not have rigid skeletons (Wing & Barnard 2004, Molodtsova 2013). The other 4 families are known as gorgonians due to their previous inclusion in the Gorgonacea order before it was subsumed into the Alcyonacea order. We included Alcyoniidae in the response variable grouping, since *H. ritteri* is commonly observed with gorgonians at SK-B and was considered a good indicator species for the other families. Tow-camera transects at SK-B from 2015 (Gale et al. 2017) observed *H. ritteri* on 7 transects along with taxa from at least one of the families Isididae (6 transects), Plexauridae (6 transects), Primnoidae (5 transects), or Paragorgiidae (4 transects). Similarly, all but one of our drop-camera observations of *H. ritteri* also had the presence of other alcyonacean coral families.

2.5. Predictor variables

We considered 6 predictor variables for species distribution modelling based on data derived from multibeam bathymetry, an ocean tidal model, and historical fishing information (Table 3). All predictor variables were converted to $100 \text{ m} \times 100 \text{ m}$ grid cell raster maps that encompassed the fishable area at SK-B Seamount (Fig. 1c). We used a Universal Transverse Mercator projection (Zone 8) for all raster layers, with a spatial extent of $41 \text{ km} \times 30 \text{ km}$ (longitudinal range: 135.9° to 135.3° W , latitudinal range: 53.2° to 53.4° N) that includes 14 896 grid cells (each $100 \text{ m} \times 100 \text{ m}$) for species distribution modelling. The grid cells for modelling were selected to encompass the primary depths (250–1350 m) where sablefish fishing occurs, excluding areas in the existing fishing closure (Fig. 1c). Since the fishing closure at the top of the seamount follows roughly the 250 fathom (457 m) contour, the majority (99.5%) of the grid cells modelled are for depths between 400 and 1350 m.

SK-B Seamount seafloor bathymetry data from the Canadian Hydrographic Services (Halcro 2000) were obtained for a $10 \text{ m} \times 10 \text{ m}$ grid and were aggregated to a $100 \text{ m} \times 100 \text{ m}$ raster using the arithmetic mean of cell values via the 'raster' package in R software version 3.5.0 (Hijmans 2017, R Core Team 2018). In addition to depth, we used bathymetric derivatives—BPI, rugosity, and slope—as predictor variables, be-

Table 3. Predictor variables used for species distribution modelling at SGaan Kinglas–Bowie Seamount

Predictor variable	Description	Source/method
Bathymetry and derivatives		
Depth (m)	10 m resolution seafloor bathymetry collected using multibeam sonar	Halcro (2000)
Bathymetric position index (BPI)	Second-order derivative of bathymetry that indicates depressions, flats, ridges, and mounds	Wright et al. (2012)
Rugosity	Ratio of contoured surface area to the area of a plane of best fit (e.g. arc:chord ratio rugosity index)	Du Preez (2015)
Slope (%)	Absolute value of vector sum of east–west and north–south gradient computed using 4 neighbouring cell method	Fleming & Hoffer (1979), Zevenbergen & Thorne (1987)
Other variables		
Maximum tidal speed (cm s ⁻¹)	Maximum predicted tidal speeds from tidal inversion software model outputs over 368 d	Egbert & Erofeeva (2002)
Cumulative fishing intensity (traps per 10 000 m ²)	Cumulative number of fishing traps deployed in 100 m × 100 m grid cells between 1991 and 2014	Derived from DFO Pacific Region groundfish catch database

cause these are typically used to identify areas with hard substrate or suitable coral habitat (Masuda & Stone 2015). Bathymetry derivatives were also calculated as rasters using 10 m × 10 m grid cells and then aggregated to 100 m × 100 m raster layers using the arithmetic mean of cell values. The BPI is a second-order derivative of bathymetry used to indicate changes in elevation associated with depressions, slopes, ridges, or mounds. A positive BPI indicates an area of higher elevation relative to the surrounding landscape (e.g. mounds, seamounts, knolls, ridges), whereas a negative BPI indicates an area of lower elevation relative to the surrounding landscape (e.g. depressions, valleys, troughs). The benthic terrain modeller extension (Wright et al. 2012) in ArcGIS was used to calculate a broad-scale BPI (inner radius of 15 m and outer radius of 30 m) raster layer. Rugosity was calculated as the contoured surface area divided by the area of a plane of best fit (i.e. arc:chord ratio [ACR] rugosity index) following the methodology in Du Preez (2015) using ArcGIS. The contoured surface area and slope (4-cell method, Fleming & Hoffer 1979) were calculated using the DEM surface tools extension (version 2.1, Jenness 2013) to ArcGIS.

Tidal speeds were obtained from the Oregon State University Tidal Inversion Software (OTIS) package (TPXO8-atlas solution, www.tpxo.net/otis) using a 100 m resolution forward solution (Egbert & Erofeeva 2002) that was parameterized using 100 m × 100 m bathymetry for SK-B Seamount and the surrounding area that includes the Hodgkins and Davidson seamounts to the north (175 km × 219 km area, longitudinal range: 137.5° to 134.1° W, latitudinal range: 52.6° to 54.1° N). Tidal speeds were generated for 1 h

intervals over 368 consecutive days to produce a tidal current time series for spring and neap tides over a complete lunar year at SK-B (Pond & Pickard 1983, Rooper et al. 2014). Maximum tidal speeds from each grid cell during the time series were used to generate the maximum tidal speed raster.

Finally, we calculated cumulative fishing intensity from the sablefish longline trap fishery at SK-B (Fisheries and Oceans Canada [DFO] groundfish database archived at the Pacific Biological Station in Nanaimo, BC) to reflect potential long-term impacts of fishing on the probability of coral presence. We assumed that traps were equally spaced in a straight line between the terminal deployment locations of sets (based on the reported surface position of the vessel) and calculated the cumulative number of traps deployed in each 100 m × 100 m grid cell from 1991 to 2014. Note that adjustments for trap bottom locations could not be made for historical trap deployments because regular fishing gear does not collect the depth sensor data needed to apply the Bayesian trap location estimator.

All predictor variable rasters were used for both model parameterization and model prediction, with the exception of depth, which was measured directly during camera deployments. Where available, we used the median of depth sensor measurements from the period that the trap was stationary on the seafloor as the observed depth when estimating model coefficients for depth. When depth sensor data were not available, we used depth data from the internal trap-camera depth sensors, and when no depth sensor data were available (3 deployments), depths were obtained from extracted bathymetry values at the surface deployment location.

2.6. Model fitting and evaluation

We fit a GAM using a binomial distribution with a logit link function for predicting the probability π_i of coral presence in each of the $i = 1, \dots, I$ 100 m × 100 m grid cells, i.e.:

$$\text{logit}(\pi_i) = \log\left(\frac{\pi_i}{1 - \pi_i}\right) = \alpha + \sum_{j=1}^p s_j(x_{ji}) + \varepsilon_i \quad (3)$$

where α is the intercept term and s_j are thin plate regression spline smoothing functions (Wood 2006) for x_j predictor variables with $j = 1, \dots, p$ (Table 3). We fit GAMs with presence/absence observations of alcyonacean corals ($n = 124$) using an all-subsets selection procedure involving all possible combinations of the $p = 6$ predictor variables. The mgcv package in R (Wood 2006) was used for GAM model fitting and the MuMIn package in R (Bartón 2019) was used for all-subsets model selection. To avoid overfitting, we weighted effective degrees of freedom by $\gamma = 1.4$ in the unbiased risk estimator (UBRE) used to estimate smoothing parameters (Kim & Gu 2004, Wood 2006), and limited degrees of freedom for the smoothing functions ($k \leq 3$ for the trap predictor and $k \leq 4$ for all other predictors, Wilborn et al. 2018). The trap predictor variable was restricted to $k \leq 3$ to avoid overfitting, as it was very sensitive to a single outlier presence observation at the maximum observed range of trap densities.

We used the Akaike information criteria corrected for small sample size (AICc, Hurvich & Tsai 1989, Burnham & Anderson 2002) to identify the model with the lowest AICc and additional candidate models that were within 2 AICc units. Models that include additional predictor variables and are within 2 AICc units of the top model are not supported if the maximized log-likelihood is essentially the same as that of the top model (Burnham & Anderson 2002). Therefore, when multiple models had AICc scores within 2 units of the lowest AICc, we selected the simplest model with the fewest predictor variables.

The data extraction process resulted in 4 datasets of presence/absence observations and environmental covariates associated with each observation based on the different estimators for the trap-camera position on the seafloor (drop location, posterior mode, posterior medoid, and posterior weighted grid cells). The GAM models and selection procedure were applied separately to each of the 4 datasets. After model selection, the environmental predictor raster layers were then used to generate predictive maps for the mean probabilities of alcyonacean coral presence at each 100 m × 100 m grid cell in the

modelled area. We computed 95 % confidence intervals for each grid cell as the mean prediction ± 1.96 SE.

We explored threshold-independent (area under the receiver operating characteristic curve [AUC], proportion of deviance explained) and threshold-dependent (kappa, percent correctly classified [PCC], specificity, sensitivity, true skill statistic [TSS]) measures for evaluating model performance (Fielding & Bell 1997, Allouche et al. 2006, Freeman & Moisen 2008a). Threshold-dependent metrics require a probability classification threshold to convert model probabilities into categorical values for presence or absence, while threshold-independent metrics do not. For example, if a threshold of 0.5 is selected for presence, then model probabilities ≥ 0.5 would be considered a predicted presence location and any probability < 0.5 would be considered an absence location. Threshold-dependent measures assess binary model classification accuracy and are derived from confusion matrices, which summarize the number of true positives (sensitivity: model correctly predicted presence where observed presences occur), false positives (model incorrectly predicted presence where observed absences occur), true negatives (specificity: model correctly predicted absence where observed absences occur), and false negatives (model incorrectly predicted absence where observed presences occur). While threshold-dependent metrics have useful applications for evaluating SDMs, such as weighting error types differently according to modelling objectives (Fielding & Bell 1997, Lobo et al. 2008), threshold-independent metrics are often preferred since they do not require the selection of a specific classification threshold.

We used 3 primary metrics to evaluate model performance:

- (1) AUC
- (2) the proportion of deviance explained (%)
- (3) the maximum kappa (κ) statistic

The AUC is a measure of total area under the receiver operating curve and is a threshold-independent measure of model accuracy since it is calculated across the entire range of possible probability thresholds for classification (0–1). The AUC estimates the probability that the model's predicted probability for a randomly selected presence observation will be greater than that for a randomly selected absence observation using ranked data (DeLong et al. 1988). General guidelines for interpreting AUC values range from poor or only marginally better than chance (0.50–0.69), acceptable (0.70–0.79), excellent (0.80–0.89), and outstanding (≥ 0.90) discrimination

(Hosmer & Lemeshow 2005). AUC is one of the most widely used metrics for evaluating SDM performance; however, one of its limitations is that it does not evaluate model goodness of fit (see Lobo et al. 2008 for other limitations on AUC). We use the proportion of null deviance explained by the model (i.e. 1 – model deviance/null deviance) as a measure of goodness of fit. The third metric used was the kappa statistic (Cohen 1960, Fielding & Bell 1997), which measures the improvement in the proportion of correctly predicted presence/absence locations over chance expectations (Manel et al. 2001). Landis & Koch (1977) suggest benchmark values of kappa that indicate slight (0.00–0.20), fair (0.21–0.40), moderate (0.41–0.60), substantial (0.61–0.80), or near-perfect (0.81–1.00) agreement between model predictions and observations. For each model, we calculated the maximum kappa statistic obtainable by varying probability thresholds between 0 and 1.

As a secondary evaluation of model performance, we assessed model binary classification accuracy over varying probability thresholds for predicting presence and absence using the PresenceAbsence package (Freeman & Moisen 2008b) implemented in R (R Core Team 2018). We identified optimal thresholds for kappa, sensitivity, specificity, PCC, TSS, and the threshold where model-predicted prevalence equals the observed prevalence of coral presence observations. The observed prevalence used was calculated from the random sampling locations.

We completed a 5-fold cross-validation for each model, where each fold uses 80% of the observations for model fitting (i.e. training data) and the remaining 20% of observations for model testing (i.e. testing data). For each of the 5 data subsets, we re-fit the model using training data only and calculated AUC and kappa test statistics using the test data that were excluded from model fitting. The 14 random samples collected during 2016 were also used to test model performance using a bootstrap procedure. We first fit the top models selected from each of the 4 datasets extracted using the different bottom location estimators, excluding the 14 random samples so they could be used as testing data. We then calculated mean AUC and kappa statistics from 100 bootstraps samples with replacement of the 14 random samples. The 14 random samples contain only 4 pres-

ence observations and, because both presence and absence data are required for diagnostics, bootstrap subsets with 0 presence observations were resampled so that all 100 bootstraps contained at least 1 presence observation.

3. RESULTS

3.1. *In situ* observations of corals and sponges

Alcyonacean corals were the most commonly observed benthic taxa group, occurring in 24% of all trap-camera sets (Table 4). Alcyonaceans were also the most diverse group, with at least 7 different taxa, including *Heteropolypus ritteri*, *Isidella* sp., *Keratoisis* sp., *Paragorgia* spp., *Parastenella* sp., Primnoidae sp., and *Swiftia simplex* (Table 5). *Parastenella* sp. and Isididae colonies were observed in the highest densities, with 34 and 10 distinct colonies, respectively, observed at single locations, while *S. simplex*, Isididae, and *H. ritteri* were observed at the most locations (Table 5). Two locations in the northeast and 1 location in the southwest had particularly high densities of alcyonaceans, with counts of 24–42 alcyonacean coral colonies of different species observed during single camera deployments at depths ranging from 550 to 866 m. Sponges (Classes Demospongiae and Hexactinellida), sea pens (Order Pennatulacea), hydrocorals (Family Stylasteridae), and black coral (Order Antipatharia) were also observed during camera deployments, but were less frequent than alcyonacean observations (Table 4).

Observed prevalence of alcyonacean corals was 20% from non-random sampling from commercial fishing sets (20 out of 99 sets), 29% for random samples (4 out of 14 sets), and 55% for ESR samples (6 out of 11 sets).

Table 4. Presence (P):absence (A) frequencies by sampling year, and total frequencies and percentages from 124 video sample sites during 2013–2016 sablefish fishing trips at SGaan Kinglas–Bowie Seamount. Note that all 2013–2015 observations are from opportunistic sampling during regular fishing sets, whereas 2016 observations include a mix of fishing, equal stratified random, and random sampling

	2013 P:A	2014 P:A	2015 P:A	2016 P:A	2013–2016 P:A	%P	%A
Corals (Order Alcyonacea)	3:9	9:45	6:20	12:20	30:94	24	76
Sponges (Phylum Porifera)	4:8	3:51	0:26	6:26	13:111	10	90
Sea whips (Order Pennatulacea)	1:11	2:52	2:24	1:31	6:118	5	95
Hydrocorals (Family Stylasteridae)	1:11	2:52	0:26	4:28	7:117	6	94
Black corals (Order Antipatharia)	1:11	0:54	0:26	3:29	4:120	3	97
Corals or sponge	6:6	12:42	8:18	15:17	41:83	33	67

Table 5. Summary of alcyonacean corals (Order Alcyonacea) observed from drop camera deployments at SGaan Kinglas–Bowie Seamount during fishing trips from 2013 to 2016

Family	Lowest taxon identified	Locations observed	Distinct colonies	Counts per set (range)	Depth range (m)
Alcyoniidae	<i>Heteropolypus ritteri</i>	6	12	1–5	721–984
Isididae	<i>Isidella</i> sp.	2	2	1	718–721
	Isididae	8	29	1–10	548–795
	<i>Keratoisis</i> sp.	1	1	1	548
Paragorgiidae	<i>Paragorgia</i> spp.	2	4	1–3	754–791
Primnoidae	<i>Parastenella</i> sp.	3	42	3–34	754–877
	Primnoidae	3	5	1–2	423–827
Plexauridae	<i>Swiftia simplex</i>	10	13	1–2	642–988
Unidentified family	Alcyonacea	20	56	1–12	423–1346

3.2. Species distribution modelling

The most prominent differences in mean predicted probabilities of presence occurred between the drop location model and posterior mode model (Fig. 3). The best-fitting models using the 4 different methods for extracting predictor data from landing position (i.e. drop, posterior mode, posterior medoid, posterior weighted) explained between 26 and 31 % of residual deviance, with mean AUC values ranging from 0.71 to 0.78 and maximum kappa values

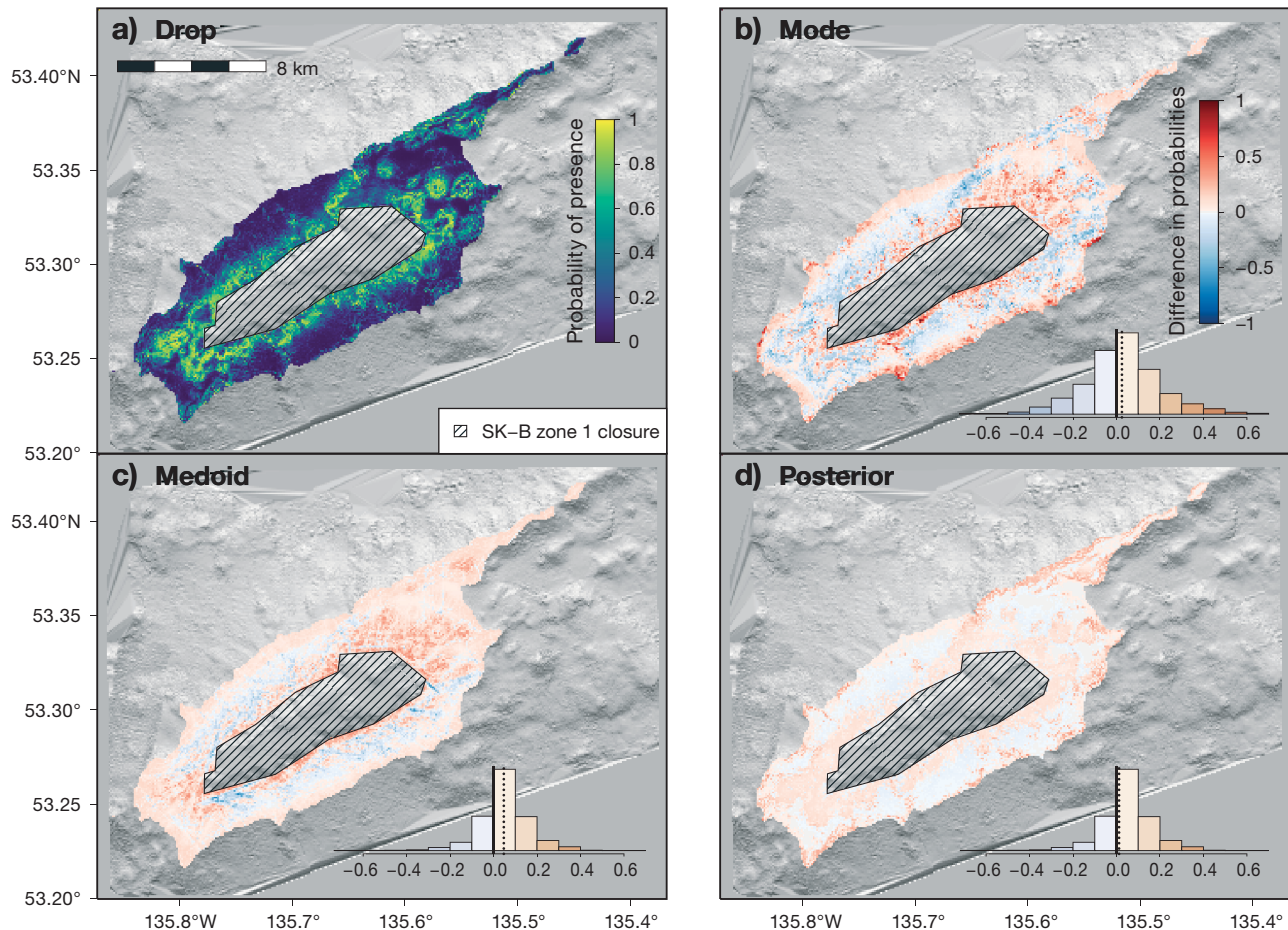


Fig. 3. (a) Mean predicted probabilities of alcyonacean corals for model using surface drop locations to extract environmental raster data used in model fitting. (b–d) Residuals from predicted probabilities between the drop location and the alternative models using environmental data estimated via (b) posterior mode position, (c) posterior medoid position, and (d) posterior weighted position. Median residual shown by vertical dotted line in the histograms. For (b–d), red colouring: locations where alternative model predicts higher probabilities than surface drop model; blue colouring: locations where alternative model predicts lower probabilities than surface drop model. SK-B: SGaan Kinglas–Bowie

Table 6. Model performance diagnostics for top models using 4 different estimators of trap-camera landing position to extract predictor data. Diagnostics shown for models fit with all observations ($n = 124$), averages from training and test datasets using 5-fold cross-validation (CV), and 100 bootstrap subsets of the 2016 random sampling locations.

Data subset	Diagnostic	Trap-camera location estimator and predictors in top model			
		Surface drop position		Posterior mode	Posterior medoid
		Depth, slope, rugosity	Depth, slope, traps	Depth, slope, rugosity, traps	Depth, slope, rugosity
All observations ($n = 124$)	R^2 adjusted	0.25	0.24	0.32	0.27
	Deviance explained (%)	0.26	0.27	0.31	0.28
	AUC (SD)	0.85 (0.04)	0.85 (0.03)	0.87 (0.04)	0.87 (0.03)
	Max. κ (SD)	0.50 (0.08)	0.49 (0.09)	0.62 (0.08)	0.51 (0.09)
	Max. κ threshold	0.26	0.32	0.30	0.40
CV training data ($n = 99.2$)	AUC (SD)	0.85 (0.04)	0.86 (0.04)	0.88 (0.04)	0.87 (0.04)
	Max. κ (SD)	0.55 (0.09)	0.53 (0.10)	0.64 (0.09)	0.55 (0.10)
	Max. κ threshold (SD)	0.30	0.34	0.34	0.33
CV test data ($n = 24.8$)	AUC (SD)	0.77 (0.11)	0.71 (0.12)	0.76 (0.11)	0.78 (0.11)
	Max. κ (SD)	0.46 (0.20)	0.36 (0.19)	0.47 (0.18)	0.46 (0.19)
	Max. κ threshold (SD)	0.34	0.32	0.30	0.28
Random samples from 2016 fishing ($n = 14$ with 100 bootstraps)	Boot mean AUC (95 % CI)	0.77 (0.50–1.00)	0.69 (0.52–0.93)	0.76 (0.51–1.00)	0.78 (0.52–1.00)
	Boot mean max. κ (95 % CI)	0.57 (0.18–1.00)	0.42 (0.06–0.81)	0.63 (0.12–1.00)	0.60 (0.20–1.00)
	Boot mean max. κ threshold	0.47	0.52	0.56	0.45

ranging from 0.36 to 0.47 for the cross-validated test datasets (Table 6). The posterior-weighted and posterior medoid models performed best, with maximum kappa in the 0.46–0.47 and 0.60–0.63 range for the cross-validated test data and bootstrapped random sample test data, respectively, indicating 'moderate' ($0.41 \leq \kappa \leq 0.60$) or 'substantial' ($0.61 \leq \kappa \leq 0.80$) agreement between model predictions and observations (Landis & Koch 1977). Posterior-weighted, posterior medoid, and drop location models had AUC scores in the 0.76–0.78 range, with 'acceptable' model performance (Hosmer & Lemeshow 2005) for both the cross-validated test data and bootstrapped random sample test data.

Depth and slope were the most important predictor variables and were retained in all of the best-fitting models, while some models also included rugosity and cumulative trap fishing as predictors (Fig. 4, Table 6). The BPI and maximum tidal speed predictor variables were not included in any of the top models selected using all-subsets model fitting with the AICc model selection criteria.

Marginal effects of the different predictors on the probability of alcyonacean presence were generated by varying the habitat variable of interest, while keeping all other variables fixed at their average observed values (Fig. 4). In all models, the depth effect leads to the greatest proportion of cells in the 400–800 m range, with high probabilities (> 40 %) of alcyonacean coral presence and lower probabilities out-

side this depth range (Fig. 5). Model uncertainty is lowest for depths between approximately 600 and 1200 m and increases for depths outside this range, which is a function of smaller sample sizes at these depths (Figs. 5d & 6). There are steep increases in the marginal probability of coral presence for slope increases between 20 and 45 % for all models; however, the changes are greatest for the drop location and posterior weighted models, which increase from 5–90 % and 3–98 %, respectively (Fig. 4). The steep slopes along the ridge in the northeast and southwest flank of the seamount produce patchy areas of high probability at depths deeper than 1000 m. Probability of presence decreases with increasing rugosity and trap numbers for the models that included those predictors. An increased proportion of grid cells with steep slopes (>30 %) and reduced trap numbers for 1100–1350 m depths relative to 800–1100 m depths, produces a small increase in the proportion of cells with probability >40 % for depths deeper than 1100 m and the bimodal shape in the density plots in Fig. 5b.

Models based on the 4 trap-camera location estimators have similar classification thresholds for generating maximum kappa (0.26–0.40) and predicted prevalence equal to observed prevalence (0.32–0.35) (Fig. 7). This is a good indicator of model accuracy, as Freeman & Moisen (2008a) found that thresholds that maximize kappa and generate predicted prevalence equal to observed prevalence have more unbiased

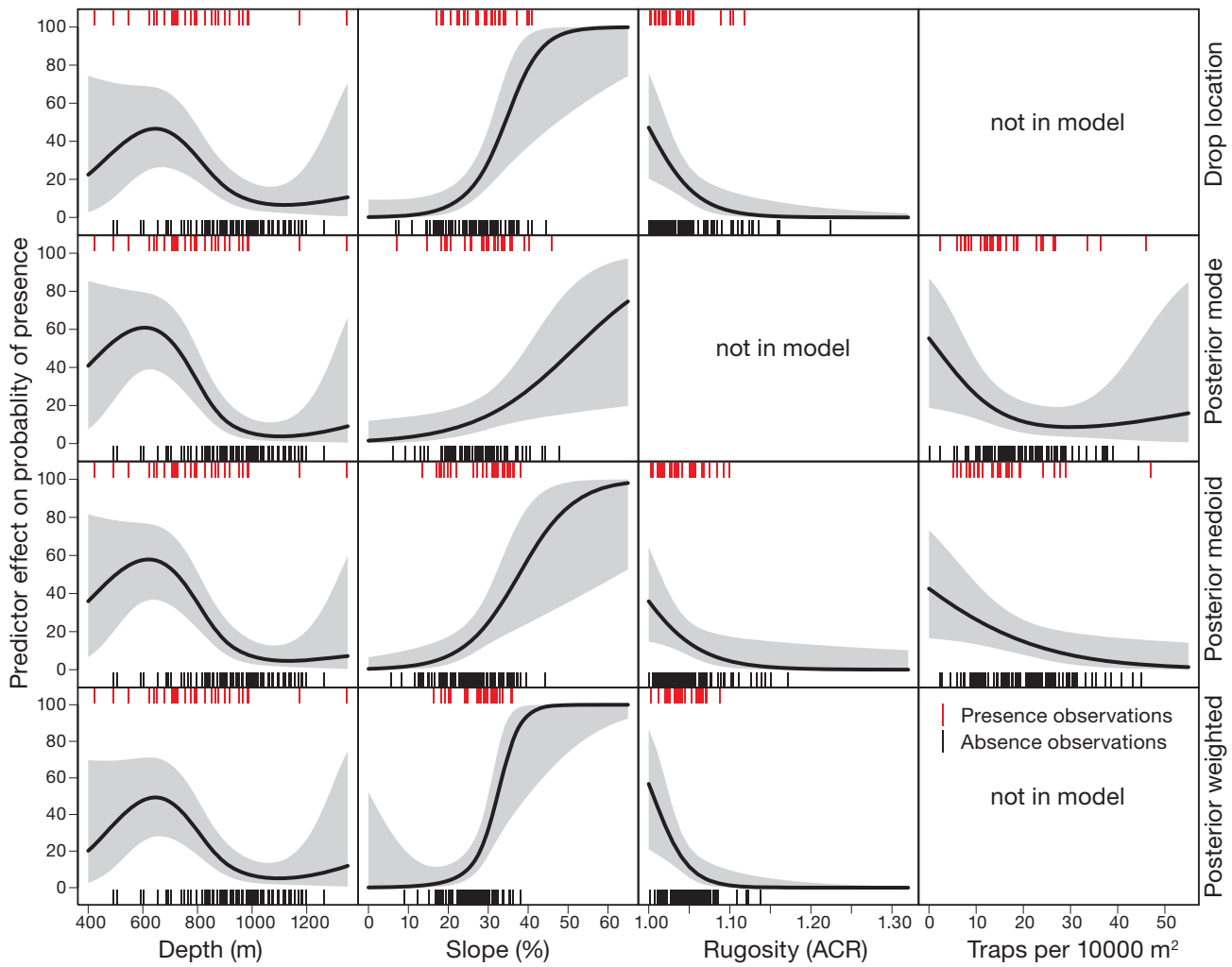


Fig. 4. Marginal effects of environmental covariates (depth, slope, rugosity, and cumulative trap fishing) on the probability of alcyonacean presence for the top selected models using alternative trap landing position estimators (1st row: drop location, 2nd row: posterior mode, 3rd row: posterior medoid, 4th row: posterior weighted). Thick black line: mean predictions; grey polygons: 95 % confidence intervals. Predictor relationships generated by varying the environmental covariate of interest, while keeping all other covariates constant at their average observed values. ACR: arc:chord ratio

maps of species prevalence and that classification thresholds for different criteria tend to converge as model quality improves. The lowest classification threshold is for sensitivity equal to specificity (0.26–0.29), while the highest threshold is for maximizing PCC (0.38–0.50). The posterior medoid model has the best performance for maximizing kappa (0.62) and PCC (85 %), compared to maximum values of 0.49–0.51 for kappa and 81–83 % PCC for the other 3 models.

Overall, the 4 models using different drop locations predicted a similar distribution of coral habitats at the seamount and a similar distribution of probabilities among the $i = 14\,896$ grid cells of size $100\text{ m} \times 100\text{ m}$ (Figs. 3 & 5a). The 4 different models predicting coral habitats with greater than 40 % probability occupy ei-

ther 31 % (drop model), 35 % (posterior mode model), 38 % (posterior medoid model), or 36 % (posterior-weighted model) of the modelled area. Differences among models occur because of the predictor variables included in the top models as well as changes to the estimated coefficients for those variables (Fig. 4). The posterior mode model has the greatest difference in probabilities relative to the drop model, with 14 % of grid cells with residuals > 0.2 (i.e. higher probability relative to drop model) and 9 % of grid cells with residuals < -0.2 (i.e. lower probability relative to drop model), that are likely related to the exclusion of the rugosity predictor and differences in fit for the slope predictor. There is less difference in predicted probabilities between the drop location, posterior-weighted model, and posterior medoid model (Fig. 3c,d). Differ-

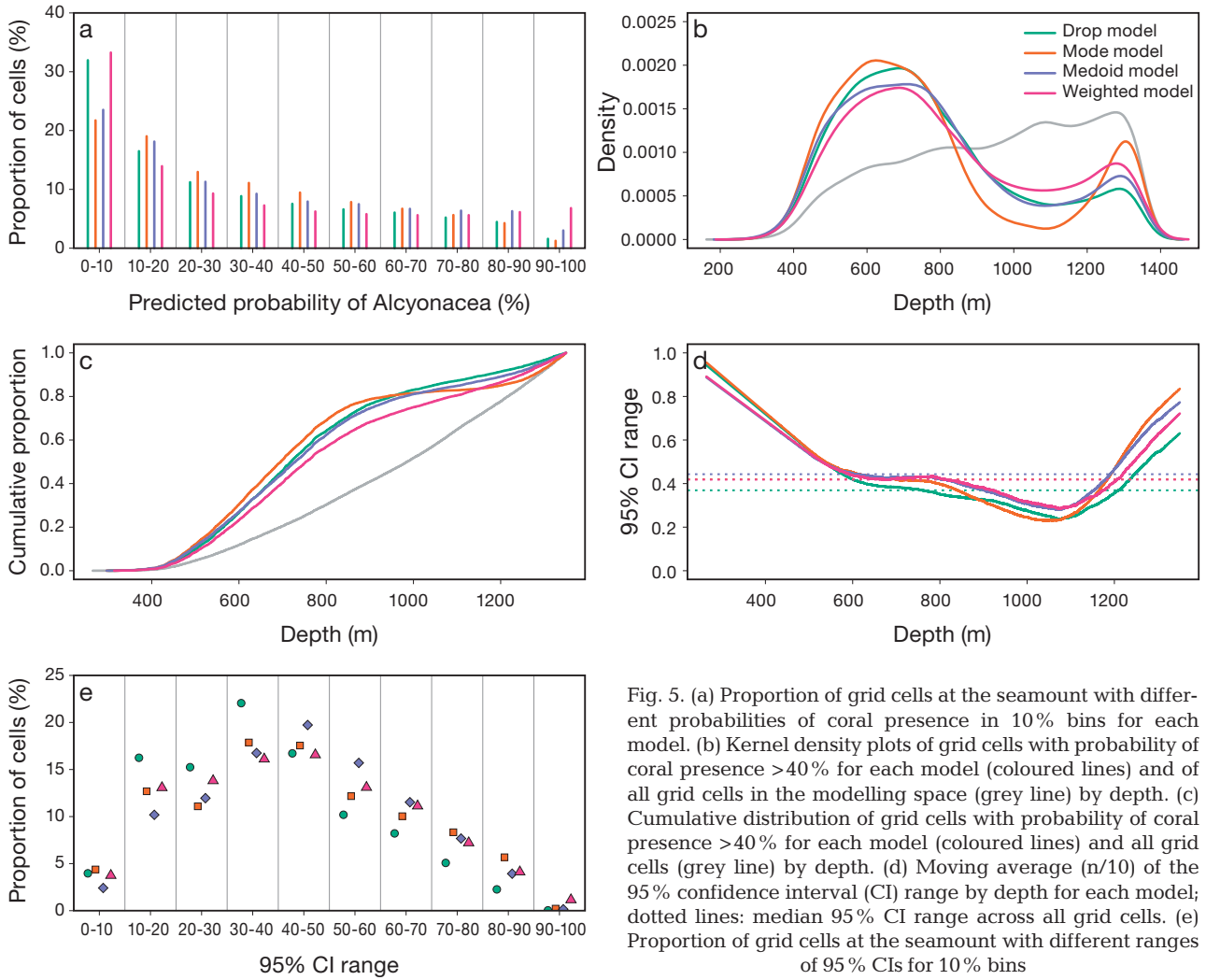


Fig. 5. (a) Proportion of grid cells at the seamount with different probabilities of coral presence in 10% bins for each model. (b) Kernel density plots of grid cells with probability of coral presence >40% for each model (coloured lines) and of all grid cells in the modelling space (grey line) by depth. (c) Cumulative distribution of grid cells with probability of coral presence >40% for each model (coloured lines) and all grid cells (grey line) by depth. (d) Moving average (n/10) of the 95% confidence interval (CI) range by depth for each model; dotted lines: median 95% CI range across all grid cells. (e) Proportion of grid cells at the seamount with different ranges of 95% CIs for 10% bins

ences between the drop and medoid models are mostly due to the inclusion of the trap predictor variable in the medoid model (Fig. 3c), as areas with higher trap density have lower probability (blue) and areas with lower trap density have higher probability (red) of coral presence in the medoid model. The posterior-weighted model and drop models include the same predictors (depth, slope, rugosity), and so their differences are solely due to changes in the coefficients for the predictors.

4. DISCUSSION

Fisheries are regularly challenged by management and eco-certification requirements to reduce risks to seafloor habitats, which requires evaluation of management strategies designed to protect habitat. Uninformed management choices threaten fisheries

sustainability and can pose conservation risks by concentrating fishing effort in smaller areas and reducing flexibility for fishing fleets to avoid non-target species or sensitive benthic habitats by moving into different areas. Due to limited information on the distribution and abundance of coral and sponge taxa in most fishing grounds, it is not possible to quantify fishing risks to these habitats or evaluate the trade-offs associated with spatial closures designed to protect them. We demonstrated a cost-efficient method for collecting *in situ* presence/absence observations of deep-water coral and sponges through the deployment of a novel deep-water camera system during routine commercial fishing activity. Our results provide useful information for spatial management of the SK-B MPA and sensitive benthic habitats in general by (1) providing spatially explicit SDMs for deep-water alcyonacean corals at the SK-B Seamount, (2) quantifying spatial uncertainty in pres-

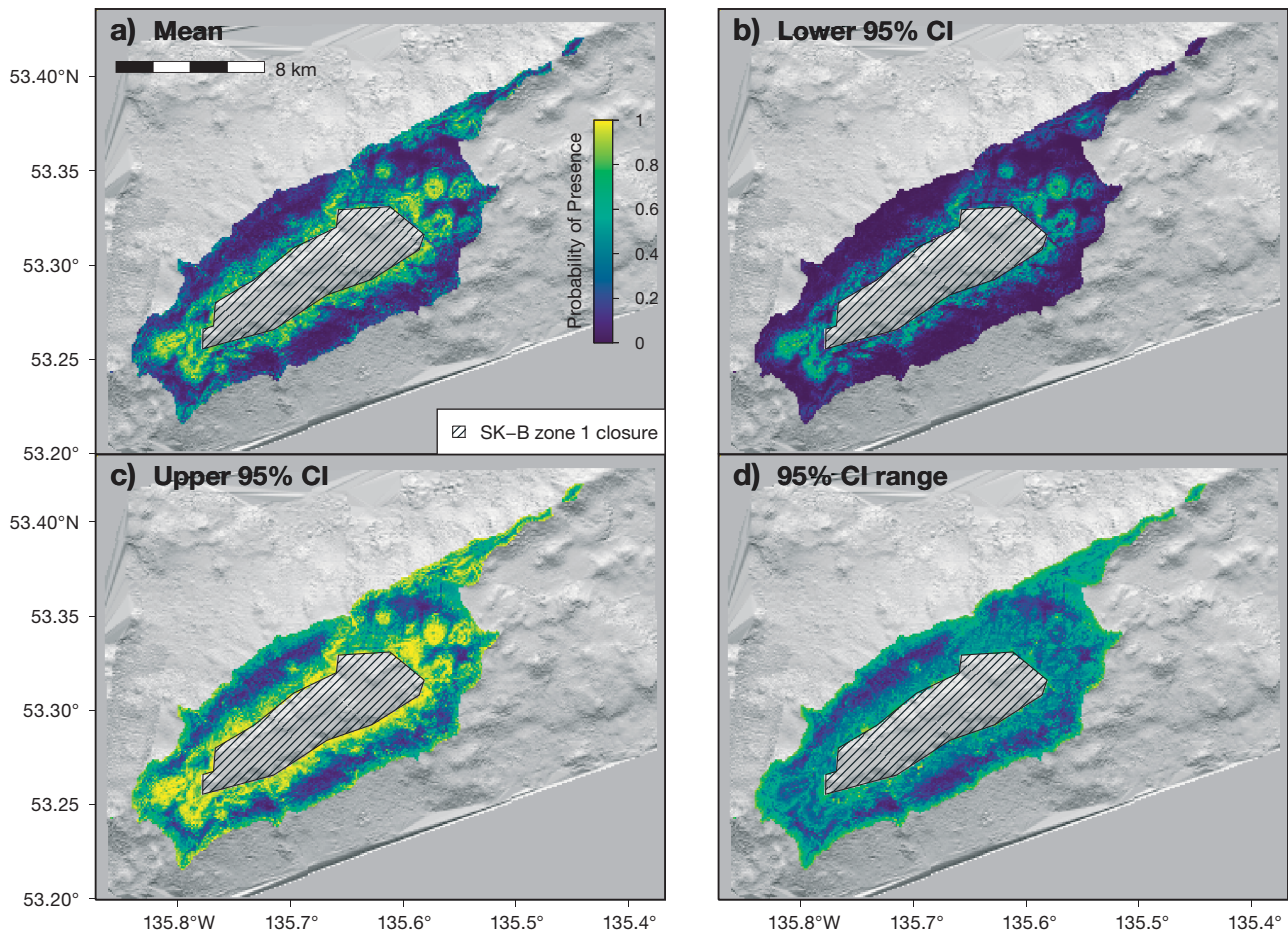


Fig. 6. Mean (a) predicted probabilities of alcyonacean presence for posterior medoid model with (b) lower, (c) upper, and (d) range for 95 % confidence intervals. SK-B: SGaan Kinglas–Bowie

ence/absence data and the implications for model variable selection and performance, (3) demonstrating the implementation of a targeted sampling programme with commercial fisheries that can improve and validate SDMs, and (4) providing a scalable framework for relatively cost-effective sampling of presence/absence data for benthic habitat over large spatial extents that cannot be easily duplicated by dedicated research activities.

4.1. Predictions for SK-B coral habitats

Despite the presence of an MPA since 2008 and fishing activity since the 1980s, information on the distribution of deep-water coral habitats at SK-B Seamount was historically limited (Etnoyer 2008, DFO 2015), as early research and data collection at the seamount focussed on catch and abundance information for target species, such as sablefish and rockfish

(Yamanaka 2005). Exploratory ROV surveys conducted in 2011 found high abundance of the coral *Primnoa pacifica* on the upper plateau of SK-B for depths between 50 and 300 m, but provided limited observations throughout the seamount for deep-water habitats of 400–1250 m where most sablefish fishing occurs (Gale et al. 2017). Only recently have observations of benthic habitats in sablefish fishing depths been collected on dedicated research trips; a tow-camera survey conducted in 2015 provided observations from 11 unique transect locations at SK-B at depths of 400–1250 m (Gale et al. 2017). Presence/absence observations of coral habitats collected through the sablefish trap-camera research programme were intended to provide broader spatial coverage and larger sample sizes that could be used to develop and validate SDMs of coral habitats within seamount fishing grounds.

Our model predictions for alcyonacean corals at SK-B Seamount suggest a large proportion of suit-

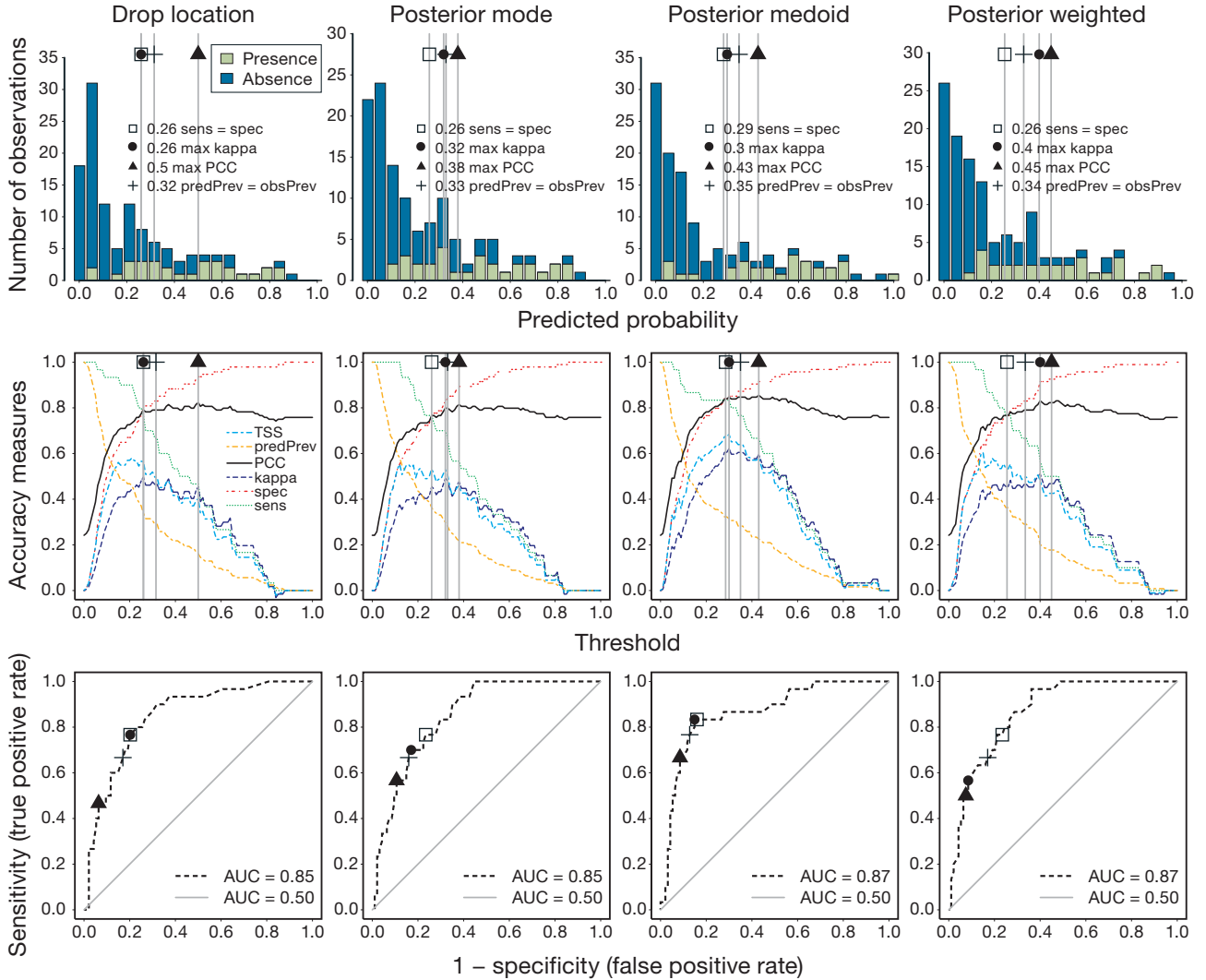


Fig. 7. Diagnostic plots for assessing candidate probability thresholds for predicting presence/absence locations of alcyonacean corals for 4 models considered ($n = 124$). Top row: histograms with the distribution of presence/absence observations for corresponding model-predicted probabilities and classification thresholds where sensitivity (sens) = specificity (spec), kappa is maximized, the percent correctly classified (PCC) observations are maximized, and predicted prevalence = observed prevalence (predPrev = obsPrev). Second row: performance of different metrics under varying probability thresholds for presence classification (TSS: true skill statistic). Third row: ROC plots for model predictions (black dashed lines) compared to what would be expected from chance (grey solid line, AUC = 0.50)

able habitat in the 400–800 m depth range with high probabilities (>0.5) of alcyonacean coral presence for areas with slopes $>30\%$. In fact, depth and slope were the most important environmental predictors for coral habitats in the top models selected, which is consistent with findings from other studies (Woodby et al. 2009, Masuda & Stone 2015). Slope may be indicative of high relief areas with hard substrate (Dunn & Halpin 2009) that is required by most corals for settlement. Areas with steeper slopes might also experience higher current flow rates or greater mixing of bottom water layers that may influence favourable conditions for coral growth by (1) providing

more food through higher rates of plankton availability and (2) limiting the settlement of suspended particles that may smother corals or reduce available substrate for new recruitment (Genin et al. 1986, Frederiksen et al. 1992, Mortensen & Buhl-Mortensen 2004, White et al. 2005). Depth is often considered a proxy for other environmental variables important for corals such as carbonate availability (used for producing carbonate skeletons), temperature, and oxygen (Woodby et al. 2009, Thresher et al. 2011, Georgian et al. 2014). Temperature of local water masses is likely a limiting factor for the shallow depth range of corals, while both food supply and tempera-

ture could be limiting factors at deeper depth ranges (Frederiksen et al. 1992, Mortensen & Buhl-Mortensen 2004, Buhl-Mortensen et al. 2015).

The 400–1000 m depth range encompasses most Alcyonacea observations from trap cameras and bycatch on sablefish fishing trips, with only 2 trap camera presence observations deeper than this (Fig. 4, Table 5) (Buchanan et al. 2015, 2017, 2018). The lower probabilities for Alcyonacea coral presence in the 800–1000 m depth range reflect a lower frequency of presence observations at these depths, which were predominantly composed of *Heteropolypus ritteri*, *Parastenella* sp., and *Swiftia simplex*. The recent ROV and tow-camera surveys at SK-B also found *H. ritteri* (738–1200 m), *Swiftia* sp. (241–1195 m), and unidentified taxa in the Primnoidae family (328–1173 m) at deeper depths (Gale et al. 2017, Gauthier et al. 2018). The latter was the most abundant and likely includes observations of *Parastenella ramosa*, which is the most commonly observed taxon in sablefish bycatch at SK-B (Buchanan et al. 2015, 2017, 2018). The 2015 ROV survey documented *Lepidisis* sp. at 816–1169 m depth and observations from the Isididae family at 330–1239 m, while our trap cameras observed Isidae in a shallower depth range of 548–795 m. The ROV/tow-camera transects also include Alcyonacea observations of shallower taxa such as *Primnoa pacifica* (242–731 m), *Paragorgia arborea* (241–863 m), and *Calcigorgia spiculifera* (201–251 m) with depth ranges extending into the fisheries closure that is excluded from the modelled grid and sampling space. Future research might evaluate how our model predictions compare with species prevalence from ROV/tow-camera transects across depths to investigate the different depth ranges observed for Isidae. Our model predictions will be reflective of the assemblage of Alcyonacea taxa within the 400–1350 m depths at SK-B and influenced by the relative abundance of certain taxa compared to others. Those taxa that occur less frequently relative to others (e.g. Family Paragorgiidae, Table 5) will have less influence on model fits. If needed for management objectives, future data collection and modelling efforts could attempt to develop models at the family, genus, or species level for the more commonly occurring habitat-forming taxa at SK-B (e.g. *Parastenella ramosa*, *Isidella* sp., *Primnoa pacifica*), which might provide more precise estimates of species prevalence across different depths and other environmental variables.

Potential probability thresholds for correctly classifying areas with presence or absence of corals were evaluated using metrics derived from confusion matrices, such as TSS, kappa, sensitivity (i.e. true

positive rate), specificity (i.e. true negative rate), and PCC. The threshold-dependent metrics suggest acceptable model classification performance over a wide range of probability thresholds between 0.26 and 0.50, depending on the model and metric, and thus there is no single 'best' threshold that can be identified for generating maps with presence/absence. The selection of a classification threshold will depend on specific objectives and tolerance for false positives, false negatives, and overall prediction accuracy. Thresholds can be adjusted to place more emphasis on reducing false positives (i.e. model predictions of coral presence where corals do not exist) or false negatives (i.e. model predictions of coral absence where corals do exist). This is directly relevant to the construction of measurable objectives from conceptual goals stated for management of sensitive benthic areas or regulated reserves, such as MPAs.

Maps with probabilities avoid the need for selecting a presence threshold and provide more information for risk assessment than assigning discrete values of presence or absence to each cell. For example, our high-resolution 100 m × 100 m probability maps can be used to rank habitat quality according to areas with the highest probability of occurrence to prioritize areas of highest conservation value as well as indicate areas with greater prediction uncertainty.

Our model predictions include 95 % confidence intervals (Fig. 6) that indicate there is greater uncertainty where there were fewer observations made (e.g. depths shallower than ~600, depths deeper than ~1200 m, and slopes >35 %). Maps of the uncertainty in probability estimates provide a diagnostic for improving model precision, whereby new sampling strategies can be implemented to improve model accuracy in cases where greater precision is needed to meet management objectives. This was the case at SK-B, where we modified the sampling design based on an evaluation of initial models fit to 2013–2015 presence/absence data to implement new sampling strategies in 2016–2017 (e.g. ESR sampling, random sampling, and improved depth coverage from regular fishing sets) to improve model performance and information for subsequent management decisions. The ESR sampling design found that initial observations from opportunistic fishing sets (2013–2015) provided limited coverage for some combinations of habitat variables (e.g. habitat strata, Table 2), suggesting that improved information for modelling might be achieved by targeted sampling of the poorly represented habitat strata. The modified 2016 sampling design improved the coverage of habitat

stratum, however; some habitat strata have fewer observations that could be targeted for future sampling. Future sampling efforts might look to increase sampling for depths between 400 and 600 m where the model predicts high probabilities of coral presence with greater uncertainty, if greater precision is needed for these areas to provide management advice. Reduced uncertainty for depths deeper than 1200 m may not be needed for management advice, as there is less fishing at these depths. The predicted probability maps for coral habitats at SK-B can be used to develop and evaluate conservation objectives for corals and sponges within a quantitative risk assessment framework. In turn, this risk assessment framework could be transportable for application to other bottom-contact fisheries and scalable to a coastwide level.

4.2. Accounting for spatial uncertainty in coral observations

Opportunistic presence-only data for deep-water habitats often have low spatial accuracy where the location of the bottom observation is only known within several kilometres. SDMs fit with presence-only bycatch data (for both mobile and fixed bottom gears) often assume an observation took place at the midpoint of the fishing event. This assumption ignores the spatial uncertainty of bycatch observations where the bycatch may have occurred anywhere along a fishing event spanning several kilometres. To account for spatial uncertainty in our trap-camera observations and extracting environmental covariates, we tested 4 different estimators for trap landing position (surface drop position and 3 Bayesian estimators). While the 4 models using different trap location estimators predict a similar distribution of corals and total proportion of the seamount with coral habitats, differences in predicted probabilities and estimated uncertainty across grid cells could affect management outcomes. For example, the posterior mode model predictions had 23 % of grid cells with probabilities ± 0.2 relative to the drop model and the range of potential coral habitat with greater than 40% probability ranged across models from 31 to 38 % (47–56 km²) of the modelling space. These finer-scale spatial differences in model predictions across different models could have meaningful implications for management measures, particularly for smaller-scale or patchy area closures designed to optimize trade-offs between habitat protection and maintaining fishing access.

The importance of the depth predictor variable in all models is likely influencing many of the similarities in predictions of coral habitats across models, since all models used the same depth predictor data and had similar depth effects on coral presence. Observed depth values for model fitting do not change between models, since depth is measured during camera deployments rather than extracted from the multibeam bathymetry raster. The other environmental predictors were extracted using the latitude and longitude coordinates of the estimated camera position on the seafloor, which varies across the 4 models and has a median distance of 218 m (0.005th quantile: 18 m, 0.995th quantile: 1020 m) from the surface drop location based on the posterior medoid estimate (see Doherty et al. 2018 for empirical distributions of bottom location estimates). Spatial autocorrelation in the other predictors might also explain similarities in performance between the 4 models, particularly if the distances over which predictors are correlated is greater than the range of spatial uncertainty (1000 m) in trap camera observations (Naimi et al. 2011). Nonetheless, differences in predictor variable values across models did influence both model variable selection (i.e. predictors included in the top model) and coefficient estimates (i.e. relationships between coral presence and predictors), both of which affected predictions for coral habitats. In our case, it appears that model variable selection had a greater effect on predictions than the coefficient estimates. The 2 models that included the same predictor variables (drop location and posterior-weighted models) had the most similar predictions for coral habitat distribution. Differences in the posterior mode and posterior medoid models are related to the exclusion of the rugosity predictor and the inclusion of the trap predictor variable, respectively. The posterior mode model also had a different fit for the slope predictor compared to other models, which could be related to the exclusion of the rugosity term and/or the bottom location coordinates used for data extraction.

For some applications, the surface drop position may provide a good enough estimator of the bottom landing position for cameras deployed in sablefish longline trap fishing gear; however, we found that the different estimators for bottom landing position affected variable selection, model performance, and model predictions for corals at SK-B. There was an improvement in model performance using the posterior-weighted and posterior medoid location models that account for spatial uncertainty in deep-water camera observations at SK-B. Greater improvements might be seen in situations where there is more spatial un-

certainty in observation locations, such as bycatch from bottom trawls spanning several kilometres or for models with larger spatial extents. This could be evaluated through simulation experiments using visual transects, such as from an ROV, where the true bottom locations of observations are known and spatial uncertainty in observation data are simulated to test performance of different model choices for estimating bottom position. Previous simulation experiments have found that increasing spatial uncertainty in observations leads to lower prediction accuracy for SDMs and that the effect of spatial uncertainty varies based on the degree of spatial autocorrelation in predictors (Naimi et al. 2011). Our results demonstrate an approach to account for spatial uncertainty in presence/absence observations and predictive variables used for SDMs. This approach could be used to improve model performance and to evaluate the implications of ignoring this uncertainty (i.e. by simulation testing different management strategies) when SDMs are used to inform management decisions.

4.3. Future opportunities for benthic habitat research and management

Using cameras deployed on commercial fishing gear to map deep-water benthic habitats over large spatial and temporal scales offers an alternative to ROVs, tow-cameras, and bycatch data traditionally available for mapping coral and sponge habitats. Deep-water video transects by ROVs or tow-cameras can collect high-resolution spatial data and high-quality video imagery of deep-sea bottom habitats, but are typically not conducted over large areas of the coast. Previous submersible, ROV, and tow-camera surveys conducted in BC have often been limited by budgets, available ship time, equipment breakdowns, and weather conditions (Yamanaka 2005, Galand 2012, Curtis et al. 2015, Gale et al. 2017). ROV or tow-camera transects are unlikely to provide the region-wide spatial coverage and large sample sizes needed for fine-scale habitat mapping in most areas where fisheries operate; they might be more effectively used to focus data collection on other useful information for habitat risk assessment (e.g. species composition, length composition, physical samples for species identification, monitoring growth/recovery, ground-truth SDMs) in conjunction with a drop-camera or trap-camera (Williams et al. 2014, Doherty et al. 2018) sampling programme designed to collect presence/absence or abundance data for SDMs over large spatial scales. Bycatch sampling

strategies might also be used in combination with cameras deployed in fishing gear to provide additional information, such as catch rates that can be used as an index of abundance (Rooper et al. 2011, 2014), and physical specimens that can assist with species identification (Buchanan et al. 2015, 2017, 2018). Ensemble modelling approaches may also be used to develop multiple models that allow use of all available datasets and produce weighted predictions (Rooper et al. 2017, Georgian et al. 2019). For example, future modelling efforts at SK-B might consider integrating multiple models using presence/absence trap-camera data, presence-only bycatch data, and ROV/tow-camera transect data (Fithian et al. 2015).

Most of the existing coral and sponge occurrence records for BC are from bycatch data collected during bottom trawling (Finney & Boutilier 2010). The current DFO database for coral and sponge occurrences has presence records from approximately 11 300 unique locations collected between 1875 and 2010 (J. Boutilier & G. Gillepsie unpubl. data), the majority of which are from bycatch records in the BC groundfish commercial trawl fishery and trawl research surveys for groundfish and invertebrates since 2001 (the year in which observers received training in coral identification; Finney & Boutilier 2010). Most areas in BC have few observations with accurate location information and lack true absence information, limiting options for generating high-resolution SDMs needed for effective management. Ideally a quantitative risk assessment approach (Welsford et al. 2014, Doherty et al. 2018) would be used for managing fishing risks to bottom habitats that (1) maps the spatial distribution of VMEs at fine spatial scales over the large areas where fisheries operate, (2) quantifies the bottom-contact area of fishing gear and the proportion of VME habitats contacted by fisheries, (3) estimates the damage or mortality rates from fishing contact with habitats to inform current status relative to some reference level (e.g. unfished biomass), and (4) estimates potential recovery or future damage to habitats over spatial and temporal scales for different management strategies (e.g. spatial closures, gear type restrictions, effort limits, move-on rules). New strategies for collecting bottom habitat information are needed to provide the essential information for steps (1) and (2), which could be achieved by deploying cameras on commercial and survey fishing sets, possibly in combination with bycatch sampling strategies.

Our trap-camera system demonstrates an alternative cost-efficient approach for collecting high-quality

presence/absence observations for corals and sponges that is scalable for mapping the large areas necessary for effective risk assessment of sensitive benthic habitats in the presence of large-scale fisheries. The trap-cameras have also been regularly deployed on the annual stratified-random coastwide survey for BC sablefish at depths of 183–1372 m, providing essential data for coastwide habitat mapping over a wide range of environmental variables. Cameras deployed on the survey have collected presence/absence video observations for corals and sponges in 291 locations between 2013 and 2017, which can be used to develop coastwide SDMs for corals and sponges, and assess bottom fishing risks to sensitive benthic habitats in coastal fisheries. Another advantage of deploying cameras on commercial fishing trips is that more observations are collected in areas with the greatest fishing effort, leading to less uncertainty in species mapping for areas that experience the greatest amount of bottom contact. There is also potential to expand this approach and deploy cameras in other bottom longline surveys or commercial fisheries on the coast. If cameras are deployed on a small fraction of commercial longline fishing or survey sets, presence/absence datasets for corals and sponges can quickly be assembled for most fishing areas and the data can be used to validate the existing model and develop more accurate SDMs for coral habitats.

Our models predict the probability of presence and absence of coral habitats only; enhanced information for assessing the probability of contact from fishing gear and the subsequent risks to corals could be obtained by developing model predictions for abundance within grid cells (i.e. grid cells with higher densities are more likely to experience higher amounts of coral mortality from fishing events). The number of colonies observed per camera deployment could be used as an index of density, or area estimates of the camera field of view could be used to measure colonies per m². Advances in camera technology and automated image analysis are rapidly opening the door for cost-efficient data collection and data processing for monitoring deep-sea ecosystems (Dawkins et al. 2013, Williams et al. 2014, Chuang et al. 2016, Dawkins et al. 2017). Moving forward, camera observations deployed during fishing might also be used to estimate density and length composition (i.e. using stereo cameras), and monitor local changes in abundance of corals and sponge populations over time for different levels of fishing effort.

The composition of corals and different species assemblages is also of interest for risk assessment, as

the probability of lethal contact from fishing gear will be affected by coral height and morphology, and subsequent recovery rates vary by species (Ewing & Kilpatrick 2014, Martin-Smith & Welsford 2014, Stephenson et al. 2019). In contrast to fish populations, corals and sponges do not move or vary distribution seasonally and are unlikely to exhibit large changes in local abundance unless impacted by extensive fishing gear or some environmental disturbance (e.g. local temperature or oxygen changes, deep-water oil spills, or introduction of other pollutants). This feature provides flexibility for sampling programmes that can allow the fishing industry or surveys to deploy cameras at sites opportunistically when they are in the area, according to predefined sampling plans that optimize sampling effort over multiple years for monitoring goals (Hirzel & Guisan 2002). Trap cameras could also be deployed regularly on fisheries independent surveys (e.g. the random-depth stratified sablefish survey in BC) to estimate changes in species prevalence and abundance to provide long-term monitoring of bottom habitats. Collaborative research partnerships with bottom-contact fisheries provide an alternative path forward for mapping and monitoring coral and sponge habitats over large spatial and temporal scales, providing the necessary information for developing and monitoring conservation objectives for benthic habitats within fisheries management plans.

4.4. Conclusion

The deployment of cameras and other sensors on commercial fishing gear provides a cost-efficient means for collecting deep-sea ecological data over the large spatial scales needed to assess fishing risks to deep-water corals and sponges. As new observations are collected during commercial fishing or surveys, sampling strategies and SDMs can be regularly updated to improve model performance and reduce uncertainty of predicted locations for sensitive benthic habitats. The collection of benthic habitat data during fishing operations means that each fishing trip has the potential to provide value in the form of (1) landings and (2) new information for VME research and management strategies to reduce risks to seafloor habitats. The improved benthic habitat data can be used to develop quantitative risk assessment frameworks for VMEs, whereby fisheries that demonstrate fishing risks to bottom habitat that are acceptably low can maintain access to fishing grounds.

Acknowledgements. We thank Wild Canadian Sablefish Ltd. (WCS) for their financial and in-kind support at all stages of this project from the initial design to field deployments and analysis. We especially thank the fishing masters who expertly deployed–retrieved camera traps on commercial fishing sets. Additional funding was provided by the NSERC Canadian Fisheries Research Network (S.P.C.), the NSERC Discovery Grants programme (S.P.C.), NSERC Canada Graduate Scholarship programme (B.D.), and the Mitacs Accelerate Cluster Grants programme (S.P.C. and WCS). This project was also made possible by Fisheries and Oceans Canada Science staff K. Castle, L. Lacko, and M. Wyeth, who assisted with camera design, data collection and preparation, equipment preparation, and training of at-sea observers. We thank 3 anonymous reviewers for helpful comments that improved the manuscript.

LITERATURE CITED

Allouche O, Tsoar A, Kadmon R (2006) Assessing the accuracy of species distribution models: prevalence, kappa and the true skill statistic (TSS). *J Appl Ecol* 43:1223–1232

Anderson OF, Guinotte JM, Rowden AA, Clark MR, Mormede S, Davies AJ, Bowden DA (2016) Field validation of habitat suitability models for vulnerable marine ecosystems in the South Pacific Ocean: implications for the use of broad-scale models in fisheries management. *Ocean Coast Manage* 120:110–126

Andrews AH, Cordes EE, Mahoney MM, Munk K, Coale KH, Cailliet GM, Heifetz J (2002) Age, growth and radiometric age validation of a deep-sea, habitat-forming gorgonian (*Primnoa resedaeformis*) from the Gulf of Alaska. *Hydrobiologia* 471:101–110

Andrews AH, Stone RP, Lundstrom CC, DeVogelaere AP (2009) Growth rate and age determination of bamboo corals from the northeastern Pacific Ocean using refined ^{210}Pb dating. *Mar Ecol Prog Ser* 397:173–185

Araújo MB, Guisan A (2006) Five (or so) challenges for species distribution modelling. *J Biogeogr* 33:1677–1688

Auster PJ, Gjerde K, Heupel E, Watling L, Grehan A, Rogers AD (2011) Definition and detection of vulnerable marine ecosystems on the high seas: problems with the ‘move-on’ rule. *ICES J Mar Sci* 68:254–264

Barnett LAK, Hennessey SM, Essington TE, Shelton AO, Feist BE, Branch TA, McClure MM (2017) Getting to the bottom of fishery interactions with living habitats: spatio-temporal trends in disturbance of corals and sponges on the US west coast. *Mar Ecol Prog Ser* 574:29–47

Bartón K (2019) MuMIn: multi-model inference. R package version 1.43.6. <https://cran.r-project.org/package=MuMIn>

Brown CJ, Smith SJ, Lawton P, Anderson JT (2011) Benthic habitat mapping: a review of progress towards improved understanding of the spatial ecology of the seafloor using acoustic techniques. *Estuar Coast Shelf Sci* 92:502–520

Buchanan S, Frey M, Keizer A (2015) SGaan Kinghlas: Bowie Seamount at-sea observer coral and sponge sample collection, May 2014. DFO Can Data Rep Fish Aquat Sci 1261

Buchanan S, Keizer A, Garter H (2017) SGaan Kinghlas: Bowie Seamount at-sea observer coral and sponge sample collection, May 2015. DFO Can Data Rep Fish Aquat Sci 1273

Buchanan S, Keizer A, Garter H (2018) SGaan Kinghlas: Bowie Seamount at-sea observer coral and sponge sample collection, May and June 2016. DFO Can Data Rep Fish Aquat Sci 1282

Buhl-Mortensen L, Olafsdottir SH, Buhl-Mortensen P, Burgos JM, Ragnarsson SA (2015) Distribution of nine cold-water coral species (Scleractinia and Gorgonacea) in the cold temperate North Atlantic: effects of bathymetry and hydrography. *Hydrobiologia* 759:39–61

Burnham K, Anderson D (2002) Model selection and multi-model inference: a practical information-theoretic approach. Springer-Verlag, New York, NY

Canessa R, Conley K, Smiley B (2003) Bowie Seamount pilot marine protected area: an ecosystem overview. *Can Tech Rep Fish Aquat Sci* 2461

Chaytor J, Keller R, Duncan R, Dziak R (2007) Seamount morphology in the Bowie and Cobb hot spot trails, Gulf of Alaska. *Geochem Geophys Geosyst* 8:Q09016

Chu JW, Leys SP (2010) High resolution mapping of community structure in three glass sponge reefs (Porifera, Hexactinellida). *Mar Ecol Prog Ser* 417:97–113

Chu JWF, Nephin J, Georgian S, Knudby A, Rooper C, Gale KSP (2019) Modeling the environmental niche space and distributions of cold-water corals and sponges in the Canadian northeast Pacific Ocean. *Deep Sea Res I* 151:103063

Chuang MC, Hwang JN, Williams K (2016) A feature learning and object recognition framework for underwater fish images. *IEEE Trans Image Process* 25:1862–1872

Clayton L, Dennison G (2017) Inexpensive video drop-camera for surveying sensitive benthic habitats: applications from glass sponge (Hexactinellida) reefs in Howe Sound, British Columbia. *Can Field Nat* 131:46–54

Cohen J (1960) A coefficient of agreement for nominal scales. *Educ Psychol Meas* 20:37–46

Conway KW, Barrie JV, Krautter M (2005) Geomorphology of unique reefs on the western Canadian shelf: sponge reefs mapped by multibeam bathymetry. *Geo-Mar Lett* 25:205–213

Curtis J, Du Preez C, Davis S, Pegg J and others (2015) 2012 expedition to Cobb Seamount: survey methods, data collections, and species observations. *Can Tech Rep Fish Aquat Sci* 3124

Davies AJ, Guinotte JM (2011) Global habitat suitability for framework-forming cold-water corals. *PLOS ONE* 6: e18483

Dawkins M, Stewart C, Gallager S, York A (2013) Automatic scallop detection in benthic environments. In: 2013 IEEE Workshop on Applications of Computer Vision, Tampa, FL. IEEE, New York, NY, p 160–167

Dawkins M, Sherrill L, Fieldhouse K, Hoogs A and others (2017) An open-source platform for underwater image and video analytics. In: 2017 IEEE Winter Conference on Applications of Computer Vision, Santa Rosa, CA. IEEE, New York, NY, p 898–906

DeLong ER, DeLong DM, Clarke-Pearson DL (1988) Comparing the areas under two or more correlated receiver operating characteristic curves: a nonparametric approach. *Biometrics* 44:837–845

DFO (Fisheries and Oceans Canada) (2015) Development of risk-based indicators for SGaan Kinghlas-Bowie Seamount Marine Protected Area using the ecological risk assessment framework. DFO Can Sci Advis Secr Sci Advis Rep 2015/054

Dichmont C, Deng A, Punt A, Ellis N and others (2008) Beyond biological performance measures in management strategy evaluation: bringing in economics and the effects of trawling on the benthos. *Fish Res* 94:238–250

Doherty B (2016) A novel technological and collaborative approach to mapping deep-sea benthic habitats and assessing risks from bottom contact fishing. Master's thesis, Simon Fraser University, Burnaby, BC

Doherty B, Cox SP (2017) Data summary of trap camera video obtained during sablefish bottom longline trap fishing at SGaan Kinglas-Bowie Seamount, 2014–2015. Can Data Rep Fish Aquat Sci 1276

↗ Doherty B, Johnson SDN, Cox SP (2018) Using autonomous video to estimate the bottom contact area of longline trap gear and presence-absence of sensitive benthic habitat. *Can J Fish Aquat Sci* 75:797–812

↗ Dolan MF, Grehan AJ, Guinan JC, Brown C (2008) Modeling the local distribution of cold-water corals in relation to bathymetric variables: adding spatial context to deep-sea video data. *Deep Sea Res I* 55:1564–1579

↗ Du Preez C (2015) A new arc-chord ratio (ACR) rugosity index for quantifying three-dimensional landscape structural complexity. *Landsc Ecol* 30:181–192

Dunham A, Mossman J, Archer S, Davies S, Pegg J, Archer E (2018) Glass sponge reefs in the Strait of Georgia and Howe Sound: status assessment and ecological monitoring advice. DFO Can Sci Advis Secr Res Doc 2018/010

↗ Dunn DC, Halpin PN (2009) Rugosity-based regional modeling of hard-bottom habitat. *Mar Ecol Prog Ser* 377:1–11

↗ Egbert GD, Erofeeva SY (2002) Efficient inverse modeling of barotropic ocean tides. *J Atmos Ocean Technol* 19: 183–204

↗ Etnoyer PJ (2008) A new species of *Isidella* bamboo coral (Octocorallia: Alcyonacea: Isididae) from northeast Pacific seamounts. *Proc Biol Soc Wash* 121:541–553

Ewing G, Kilpatrick R (2014) Estimating the gear footprint of demersal trawl and longline fishing gears used in the Heard Island and McDonald Islands fisheries. In: Welsford DC, Ewing GP, Constable AJ, Hibberd T, Kilpatrick R (eds) Demersal fishing interactions with marine benthos in the Australian EEZ of the Southern Ocean: an assessment of the vulnerability of benthic habitats to impact by demersal gears. Department of the Environment, Australian Antarctic Division and FRDC, Kingston, Tasmania, p 176–198

Ewing G, Hibberd T, Welsford D (2014) Assessing the resistance of vulnerable benthic taxa to disturbance from demersal fishing in the HIMI region. In: Welsford DC, Ewing GP, Constable AJ, Hibberd T, Kilpatrick R (eds) Demersal fishing interactions with marine benthos in the Australian EEZ of the Southern Ocean: an assessment of the vulnerability of benthic habitats to impact by demersal gears. Department of the Environment, Australian Antarctic Division and FRDC, Kingston, Tasmania, p 226–246

↗ Fielding AH, Bell JF (1997) A review of methods for the assessment of prediction errors in conservation presence/absence models. *Environ Conserv* 24:38–49

Finney JL (2009) Overlap of predicted cold-water coral habitat and bottom-contact fisheries in British Columbia. Master's thesis, Simon Fraser University, Burnaby, BC

Finney JL, Boutilier P (2010) Distribution of cold-water coral, sponges and sponge reefs in British Columbia with options for identifying significant encounters. DFO Can Sci Advis Secr Res Doc 2010/090

↗ Fithian W, Elith J, Hastie T, Keith DA (2015) Bias correction in species distribution models: pooling survey and collection data for multiple species. *Methods Ecol Evol* 6: 424–438

Fleming MD, Hoffer RM (1979) Machine processing of Landsat MSS data and DMA topographic data for forest cover type mapping. *LARS Tech Reports*:80

↗ Frederiksen R, Jensen A, Westerberg H (1992) The distribution of the scleractinian coral *Lophelia pertusa* around the Faroe Islands and the relation to internal tidal mixing. *Sarsia* 77:157–171

↗ Freeman EA, Moisen GG (2008a) A comparison of the performance of threshold criteria for binary classification in terms of predicted prevalence and kappa. *Ecol Modell* 217:48–58

↗ Freeman EA, Moisen G (2008b) PresenceAbsence: an R package for presence absence analysis. *J Stat Softw* 23:1–31

Galand LA (2012) Bottom trawling impacts on diversity and composition of habitat-forming benthic communities in Hecate Strait, British Columbia. Master's thesis, Simon Fraser University, Burnaby, BC

Gale KSP, Curtis JMR, Morgan KH, Stanley C and others (2017) Survey methods, data collections, and species observations from the 2015 survey to SGaan Kinglas-Bowie Marine Protected Area. *Can Tech Rep Fish Aquat Sci* 3206

Gass SE, Willison JM (2005) An assessment of the distribution of deep-sea corals in Atlantic Canada by using both scientific and local forms of knowledge. In: Freiwald A, Roberts, JM (eds) *Cold-water corals and ecosystems*. Springer, Berlin, p 223–245

Gauthier M, Curtis JMR, Gale KSP, Archer SK, Haggarty DR (2018) SGaan Kinglas-Bowie Seamount Marine Protected Area species inventory: algae, Bryozoa, Cnidaria, and Porifera. *Can Tech Rep Fish Aquat Sci* 3196

↗ Genin A, Dayton PK, Lonsdale PF, Spiess FN (1986) Corals on seamount peaks provide evidence of current acceleration over deep-sea topography. *Nature* 322:59–61

↗ Georgian SE, Shedd W, Cordes EE (2014) High-resolution ecological niche modelling of the cold-water coral *Lophelia pertusa* in the Gulf of Mexico. *Mar Ecol Prog Ser* 506:145–161

↗ Georgian SE, Anderson OF, Rowden AA (2019) Ensemble habitat suitability modeling of vulnerable marine ecosystem indicator taxa to inform deep-sea fisheries management in the South Pacific Ocean. *Fish Res* 211:256–274

Government of Canada (2008) Regulatory impact analysis statement. *Can Gaz II* 142:1041–1055

↗ Graham CH, Elith J, Hijmans RJ, Guisan A, Peterson AT, Loiselle BA (2008) The influence of spatial errors in species occurrence data used in distribution models. *J Appl Ecol* 45:239–247

↗ Guillera-Arroita G, Lahoz-Monfort JJ, Elith J (2014) Maxent is not a presence-absence method: a comment on Thibaud et al. *Methods Ecol Evol* 5:1192–1197

↗ Guinan J, Brown C, Dolan MF, Grehan AJ (2009) Ecological niche modelling of the distribution of cold-water coral habitat using underwater remote sensing data. *Ecol Inform* 4:83–92

↗ Guisan A, Zimmermann NE (2000) Predictive habitat distribution models in ecology. *Ecol Modell* 135:147–186

Halcro K (2000) July/August trip report: Pacific report, NOAA Ship Rainier, Kodiak Island area, Bowie & Hodgkins seamounts. Canadian Hydrographic Service, DFO, Institute of Ocean Sciences, Sidney, BC

↗ Hastie T, Fithian W (2013) Inference from presence-only data: the ongoing controversy. *Ecography* 36:864–867

↗ Heifetz J (2002) Coral in Alaska: distribution, abundance, and species associations. *Hydrobiologia* 471:19–28

➤ Hijmans RJ (2017) raster: geographic data analysis and modeling. R package version 2.6-7. <https://cran.r-project.org/package=raster>

➤ Hirzel A, Guisan A (2002) Which is the optimal sampling strategy for habitat suitability modelling. *Ecol Model* 157:331–341

Hosmer DW, Lemeshow S (2005) Assessing the fit of the model in applied logistic regression, 2nd edn. John Wiley & Sons, Hoboken, NJ

➤ Hurvich CM, Tsai CL (1989) Regression and time series model selection in small samples. *Biometrika* 76:297–307

➤ Iturbide M, Bedia J, Herrera S, Hierro O del, Pinto M, Gutiérrez JM (2015) A framework for species distribution modelling with improved pseudo-absence generation. *Ecol Model* 312:166–174

➤ Jenness J (2013) DEM Surface Tools. Jenness Enterprises. www.jennessent.com/arcgis/surface_area.htm

➤ Kim YJ, Gu C (2004) Smoothing spline Gaussian regression: more scalable computation via efficient approximation. *J R Stat Soc B* 66:337–356

➤ Kinlan BP, Poti M, Drohan AF, Packer DB, Dorfman DS, Nizinski MS (2020) Predictive modeling of suitable habitat for deep-sea corals offshore the northeast United States. *Deep Sea Res I* 158:103229

➤ Krieger KJ, Wing BL (2002) Megafauna associations with deepwater corals (*Primnoa* spp.) in the Gulf of Alaska. *Hydrobiologia* 471:83–90

➤ Lagasse CR, Knudby A, Curtis J, Finney JL, Cox SP (2015) Spatial analyses reveal conservation benefits for cold-water corals and sponges from small changes in a trawl fishery footprint. *Mar Ecol Prog Ser* 528:161–172

➤ Landis JR, Koch GG (1977) The measurement of observer agreement for categorical data. *Biometrics* 33:159–174

➤ Lobo JM, Jiménez-Valverde A, Real R (2008) AUC: a misleading measure of the performance of predictive distribution models. *Glob Ecol Biogeogr* 17:145–151

➤ Manel S, Williams HC, Ormerod SJ (2001) Evaluating presence-absence models in ecology: the need to account for prevalence. *J Appl Ecol* 38:921–931

Martin-Smith K, Welsford D (2014) Assessing the relative vulnerability to disturbance of benthic, habitat-forming organisms in the Southern Ocean using a global database of life history characteristics and environmental correlates. In: Welsford DC, Ewing GP, Constable AJ, Hibberd T, Kilpatrick R (eds) Demersal fishing interactions with marine benthos in the Australian EEZ of the Southern Ocean: an assessment of the vulnerability of benthic habitats to impact by demersal gears. Department of the Environment, Australian Antarctic Division and FRDC, Kingston, Tasmania, p 65–85

➤ Masuda MM, Stone RP (2015) Bayesian logistic mixed-effects modelling of transect data: relating red tree coral presence to habitat characteristics. *ICES J Mar Sci* 72: 2674–2683

➤ Mercier A, Hamel JF (2011) Contrasting reproductive strategies in three deep-sea octocorals from Eastern Canada: *Primnoa resedaeformis*, *Keratoisis ornata*, and *Anthomastus grandiflorus*. *Coral Reefs* 30:337–350

➤ Molodtsova TN (2013) Deep-sea mushroom soft corals (Octocorallia: Alcyonacea: Alcyoniidae) of the northern Mid-Atlantic Ridge. *Mar Biol Res* 9:488–515

➤ Mortensen PB, Buhl-Mortensen L (2004) Distribution of deep-water gorgonian corals in relation to benthic habitat features in the Northeast Channel (Atlantic Canada). *Mar Biol* 144:1223–1238

➤ Naimi B, Skidmore AK, Groen TA, Hamm NA (2011) Spatial autocorrelation in predictors reduces the impact of positional uncertainty in occurrence data on species distribution modelling. *J Biogeogr* 38:1497–1509

➤ Neves BM, Du Preez C, Edinger E (2014) Mapping coral and sponge habitats on a shelf-depth environment using multibeam sonar and ROV video observations: Learmonth Bank, northern British Columbia, Canada. *Deep Sea Res II* 99:169–183

➤ Penney AJ, Guinotte JM (2013) Evaluation of New Zealand's high-seas bottom trawl closures using predictive habitat models and quantitative risk assessment. *PLOS ONE* 8:e82273

➤ Phillips SJ, Elith J (2013) On estimating probability of presence from use-availability or presence-background data. *Ecology* 94:1409–1419

➤ Phillips SJ, Dudík M, Schapire RE (2004) A maximum entropy approach to species distribution modeling. In: Proceedings of the 21st International Conference on Machine Learning, Banff, Canada. Association for Computing Machinery, New York, NY, p 655–662

➤ Phillips SJ, Dudík M, Elith J, Graham CH, Lehmann A, Leathwick J, Ferrier S (2009) Sample selection bias and presence-only distribution models: implications for background and pseudo-absence data. *Ecol Appl* 19:181–197

➤ Pitcher CR, Ellis N, Venables WN, Wassenberg TJ and others (2015) Effects of trawling on sessile megabenthos in the Great Barrier Reef and evaluation of the efficacy of management strategies. *ICES J Mar Sci* 73:i115–i126

➤ Pitcher CR, Ellis N, Jennings S, Hiddink JG and others (2017) Estimating the sustainability of towed fishing-gear impacts on seabed habitats: a simple quantitative risk assessment method applicable to data-limited fisheries. *Methods Ecol Evol* 8:472–480

Pond S, Pickard GL (1983) Introductory dynamical oceanography. Butterworth-Heinemann, Oxford

R Core Team (2018) R: a language and environment for statistical computing. R Foundation for Statistical Computing, Vienna

➤ Rengstorf AM, Grehan A, Yesson C, Brown C (2012) Towards high-resolution habitat suitability modeling of vulnerable marine ecosystems in the deep-sea: resolving terrain attribute dependencies. *Mar Geod* 35:343–361

➤ Rooper CN, Wilkins ME, Rose CS, Coon C (2011) Modeling the impacts of bottom trawling and the subsequent recovery rates of sponges and corals in the Aleutian Islands, Alaska. *Cont Shelf Res* 31:1827–1834

➤ Rooper CN, Zimmermann M, Prescott MM, Hermann AJ (2014) Predictive models of coral and sponge distribution, abundance and diversity in bottom trawl surveys of the Aleutian Islands, Alaska. *Mar Ecol Prog Ser* 503:157–176

➤ Rooper CN, Sigler MF, Goddard P, Malecha P and others (2016) Validation and improvement of species distribution models for structure-forming invertebrates in the eastern Bering Sea with an independent survey. *Mar Ecol Prog Ser* 551:117–130

➤ Rooper CN, Zimmermann M, Prescott MM (2017) Comparison of modeling methods to predict the spatial distribution of deep-sea coral and sponge in the Gulf of Alaska. *Deep Sea Res I* 126:148–161

➤ Rowden AA, Anderson OF, Georgian SE, Bowden DA, Clark MR, Pallentin A, Miller A (2017) High-resolution habitat suitability models for the conservation and management of vulnerable marine ecosystems on the Louisville Seamount Chain, South Pacific Ocean. *Front Mar Sci* 4:335

Sainsbury KJ, Campbell RA, Lindholm R, Whitelaw AW (1997) Experimental management of an Australian multispecies fishery: examining the possibility of trawl-induced habitat modification. In: Pikitch EK, Huppert DD, Sissenwine MP (eds) Global trends: fisheries management. Proc 20th American Fisheries Society Symposium, American Fisheries Society, Bethesda, MD, p 107–112

↳ Sigler MF, Rooper CN, Hoff GR, Stone RP, McConaughey RA, Wilderbuer TK (2015) Faunal features of submarine canyons on the eastern Bering Sea slope. *Mar Ecol Prog Ser* 526:21–40

↳ Stephenson F, Bulmer RH, Meredyth-Young M, Meysick L, Hewitt JE, Lundquist CJ (2019) Effects of benthic protection extent on recovery dynamics of a conceptual seafloor community. *Front Mar Sci* 6:1–15

↳ Thresher RE, Tilbrook B, Fallon S, Wilson NC, Adkins J (2011) Effects of chronic low carbonate saturation levels on the distribution, growth and skeletal chemistry of deep-sea corals and other seamount megabenthos. *Mar Ecol Prog Ser* 442:87–99

↳ Turner DL, Jarrard RD, Forbes RB (1980) Geochronology and origin of the Pratt-Welker seamount chain, Gulf of Alaska: a new pole of rotation for the Pacific plate. *J Geophys Res* 85:6547–6556

↳ Vierod AD, Guinotte JM, Davies AJ (2014) Predicting the distribution of vulnerable marine ecosystems in the deep sea using presence-background models. *Deep Sea Res II* 99:6–18

↳ Waller RG, Stone RP, Johnstone J, Mondragon J (2014) Sexual reproduction and seasonality of the Alaskan red tree coral, *Primnoa pacifica*. *PLOS ONE* 9:e90893

Watling L, Auster PJ (2005) Distribution of deep-water Alcyonacea off the northeast coast of the United States. In: Freiwald A, Roberts JM (eds) Cold-water corals and ecosystems. Springer, Berlin, p 279–296

Welsford D, Sumner M, Ewing G (2014) Estimates of the multi-gear footprint of the toothfish fishery at HIMI. In: Welsford DC, Ewing GP, Constable AJ, Hibberd T, Kilpatrick R (eds) Demersal fishing interactions with marine benthos in the Australian EEZ of the Southern Ocean: an assessment of the vulnerability of benthic habitats to impact by demersal gears. Department of the Environment, Australian Antarctic Division and FRDC, Kingston, Tasmania, p 199–210

White M, Mohn C, de Stigter H, Mottram G (2005) Deep-water coral development as a function of hydrodynamics and surface productivity around the submarine banks of the Rockall Trough, NE Atlantic. In: Friewald A, Roberts J (eds) Cold-water corals and ecosystems. Springer, Berlin, p 503–514

↳ Wilborn R, Rooper CN, Goddard P, Li L, Williams K, Towler R (2018) The potential effects of substrate type, currents, depth and fishing pressure on distribution, abundance, diversity, and height of cold-water corals and sponges in temperate, marine waters. *Hydrobiologia* 811:251–268

↳ Williams A, Schlacher TA, Rowden AA, Althaus F and others (2010) Seamount megabenthic assemblages fail to recover from trawling impacts. *Mar Ecol* 31:183–199

↳ Williams K, De Robertis A, Berkowitz Z, Rooper C, Towler R (2014) An underwater stereo-camera trap. *Methods Oceanogr* 11:1–12

Wing BL, Barnard DR (2004) A field guide to Alaskan corals. NOAA Tech Memo NMFS-AFSC-146

↳ Winship A, Thorson J, Clarke ME, Coleman HM and others (2020) Good practices for species distribution modeling of deep-sea corals and sponges for resource management: data collection, analysis, validation, and communication. *Front Mar Sci* 7:303

Wood SN (2006) Generalized additive models: an introduction with R. Chapman & Hall, CRC Press, Boca Raton, FL

↳ Woodby D, Carlile D, Hulbert L (2009) Predictive modeling of coral distribution in the Central Aleutian Islands, USA. *Mar Ecol Prog Ser* 397:227–240

↳ Wright DJ, Pendleton M, Boulware J, Walbridge S and others (2012) ArcGIS Benthic Terrain Modeler (BTM) v. 3.0. Environmental Systems Research Institute, NOAA Coastal Services Center, Massachusetts Office of Coastal Zone Management

Yamanaka KL (2005) Data report for the research cruise onboard the CCGS John P. Tully and the F/V Double Decker to Bowie Seamount and Queen Charlotte Islands July 31st to August 14th 2000. Can Data Rep Fish Aquat Sci 1163

Zevenbergen LW, Thorne CR (1987) Quantitative analysis of land surface topography. *Earth Surf Process Landforms* 12:47–56

Editorial responsibility: Jean-Sébastien Lauzon-Guay,
Dartmouth, Nova Scotia, Canada

Reviewed by: T. Hourigan and 2 anonymous referees

Submitted: January 3, 2020

Accepted: November 3, 2020

Proofs received from author(s): February 1, 2021